Applied Geochemistry 111 (2019) 104425

Contents lists available at ScienceDirect

Applied Geochemistry

journal homepage: http://www.elsevier.com/locate/apgeochem

GEMAS: Geochemical background and mineral potential of emerging tech-critical elements in Europe revealed from low-sampling density geochemical mapping☆

Philippe Négrel [a,*], Anna Ladenberger [b], Clemens Reimann [c], Manfred Birke [d], Alecos Demetriades [e], Martiya Sadeghi [b], The GEMAS Project Team1

[a] BRGM, Water, Environment, Process Development and Analysis Division, Orléans, France
[b] Geological Survey of Sweden, Uppsala, Sweden
[c] Geological Survey of Norway, Trondheim, Norway
[d] Bundesanstalt für Geowissenschaften und Rohstoffe, Stillweg 2, 30655, Hannover, Germany
[e] Institute of Geology and Mineral Exploration, 1 Spirou Louis St., Olympic Village, Acharnae, 13677, Athens, Hellenic Republic

ARTICLE INFO

Editorial handling by de Caritat Patrice

Keywords:
Agricultural soil
Weathering
Geochemistry
Critical elements
Antimony
Tungsten
Lithium

ABSTRACT

The demand for 'high-tech' element resources (e.g., rare earth elements, lithium, platinum group elements) has increased with their continued consumption in developed countries and the emergence of developing economies. To provide a sound knowledge base for future generations, it is necessary to identify the spatial distribution of critical elements at a broad-scale, and to delineate areas for follow-up surveys. Subsequently, this knowledge can be used to study possible environmental consequences of the increased use of these resources.

In this paper, three critical industrial elements (Sb, W, Li) from low-sampling density geochemical mapping at the continental-scale are presented. The geochemical distribution and spatial patterns have been obtained from agricultural soil samples (Ap-horizon, 0–20 cm; N = 2108 samples) collected at a density of 1 site per 2500 km^2 and analysed by ICP-MS after a hot aqua regia digestion as part of the GEMAS (GEochemical Mapping of Agricultural and grazing land Soil) soil-mapping project in 33 European countries. Most of the geochemical maps show exclusively natural background element concentrations with minor, or without, anthropogenic influence. The maximum extent of the last glaciation is marked as a discrete element concentration break, and a distinct difference occurs in element concentration levels between the soil of northern and southern Europe, most likely an effect of soil genesis, age and weathering. The Sb, W and Li concentrations in soil provide a general overview of element spatial distribution in relation to complexity of the underlying bedrock and element mobility in the surface environment at the continental-scale. The chemical composition of agricultural soil represents largely the primary mineralogy of the source bedrock, the effects of pre- and post-depositional chemical weathering, formation of secondary products, such as clays, and element mobility, either by leaching or mineral sorting. Observed geochemical patterns of Li, W and Sb can be often linked with known mineralisation as recorded in the ProMine Mineral Database, where elements in question occur either as main or secondary resources. Anthropogenic impact has only been identified locally, predominantly in the vicinity of large urban agglomerations. Unexplained high element concentrations may potentially indicate new sources for high-tech elements and should be investigated at a more detailed scale.

☆ Note: All web links checked on the 9th March 2019

* Corresponding author.
E-mail addresses: p.negrel@brgm.fr (P. Négrel), anna.ladenberger@sgu.se (A. Ladenberger), clemensreimann@yahoo.co.uk (C. Reimann), Manfred.Birke@bgr.de (M. Birke), alecos.demetriades@gmail.com (A. Demetriades), martiya.sadeghi@sgu.se (M. Sadeghi).

[1] The GEMAS Project Team: S. Albanese, M. Andersson, R. Baritz, M.J. Batista, B. Flem, A. Bel-lan, D. Cicchella, B. De Vivo, W. De Vos, E. Dinelli, M. Ďuriš, A. Dusza-Dobek, O.A. Eggen, M. Eklund, V. Ernstsen, P. Filzmoser, D.M.A. Flight, S. Forrester, M. Fuchs, U. Fügedi, A. Gilucis, M. Gosar, V. Gregorauskiene, W. De Groot, A. Gulan, J. Halamić, E. Haslinger, P. Hayoz, R. Hoffmann, J. Hoogewerff, H. Hrvatovic, S. Husnjak, L. Janik, G. Jordan, M. Kaminari, J. Kirby, J. Kivisilla, V. Klos, F. Krone, P. Kwećko, L. Kuti, A. Lima, J. Locutura, D.P. Lucivjansky, A. Mann, D. Mackovych, J. Matschullat, M. McLaughlin, B.I. Malyuk, R. Maquil, R.G. Meuli, G. Mol, P.O'Connor, R.K. Oorts, R.T. Ottesen, A. Pasieczna, W. Petersell, S. Pfleiderer, M. Poňavič, S. Pramuka, C. Prazeres, U. Rauch, S. Radusinović, I. Salpeteur, R. Scanlon, A. Schedl, A.J. Scheib, I. Schoeters, P. Šefčik, E. Sellersjö, F. Skopljak, I. Slaninka, A. Šorša, R. Srvkota, T. Stafilov, T. Tarvainen, V. Trendavilov, P. Valera, V. Verougstraete, D. Vidojević, A. Zissimos, Z. Zomeni.

https://doi.org/10.1016/j.apgeochem.2019.104425
Received 16 April 2019; Received in revised form 23 September 2019; Accepted 23 September 2019
Available online 24 September 2019
0883-2927/

1. Introduction

The demands for a variety of mineral and/or element resources (rare earth elements, platinum group elements, cobalt, beryllium, lithium, iodine, etc.) are strongly increasing (Buchert et al., 2009; Bertrand et al., 2016; Meinert et al., 2016). These elements are essential for maintaining and improving the present and future quality of life, including many high-technology yet low-carbon industries. Two factors have been used by the National Research Council (NRC) to rank criticality: (a) the degree to which a commodity is essential and (b) the risk of supply disruption for the commodity (Ali et al., 2017). Further, the demand for energy-related minerals has increased, as global energy production diversifies beyond carbon and nuclear-based sources (Teske, 2019). Many of these elements are crucial to a variety of manufacturing, high-tech and military applications like photovoltaic solar cells (Ga, Ge, In, Se, Ag, Te), high-strength permanent magnets and magnetic and/or optical components for lighting (mostly rare earth elements and Co), for wind turbines and hybrid automobiles, high performance batteries (Li, La), catalysts (Pt, Pd, Ce), advanced turbines (Re), and advanced energy reactor designs (He). A critical mineral and/or element is both essential in use, subject to the risk of supply restriction and the induction of environmental impacts. Based on information about occurrences, resources and reserves, extraction, processing, utilisation, and recycling, good candidates for the designation of 'energy-critical' elements can be determined. The list of critical raw materials (Table 1) is updated by the European Union Commission every few years with the last update in 2017 (European Commission, 2017).

The overall results of the 2017 criticality assessment are shown in Fig. 1 where the critical raw materials are denoted by the red dots (European Commission, 2017). Of the 61 candidate raw materials assessed (58 individual and 3 grouped materials, biotic and abiotic), the following 26 raw materials and groups of raw materials were identified as critical (Table 1). It is noted that Li discussed here is not yet a critical raw material, according to the 2017 European Commission classification, but its criticality is being discussed in view of its importance as a critical element for future sustainable technologies according to UNEP (2009). Lithium is an essential, in fact a critical, element in the battery industry and in technical evolution towards low-carbon society.

Geoscientists have a prominent role in the exploration for, management of, and environmentally safe handling of critical mineral and/or element resources considering that these needs will become even more important as the world's population and standards of living continue to increase (Nickless et al., 2015; Ali et al., 2017). It is worth noting that the concept of criticality is variable (and to large degree political) and depends principally on the context. What is critical for a state, a manufacturer or a product may not be critical for another, and what is critical for national defence may be different when compared to what is necessary to make an electronic apparatus cheaper. Therefore, prioritisation of critical minerals and/or elements are crucial for modern societies and has important implications for our economic prosperity (Bringezu et al., 2016).

To provide a solid resource base for the future, but also to timely identify any possible new environmental impact of the increased use of these elements, it is necessary to identify their natural spatial distribution with a wider view, from the order of a country or a continental block, e.g., European Union (Lambert et al., 2013). Any significant change in their cycle at the Earth's surface, due to their increased use in a variety of technological applications, needs robust preliminary knowledge. The growing consumption of critical elements generates the demand for new production, both from primary (ore deposits) and secondary (mineral-based and non-mineral-based wastes) sources. At some point, they may become new contaminants and their identification in various environmental compartments is an urgent issue for future pollution and waste management.

Table 1
List of Critical Raw Materials, updated in 2017 by the European Commission (2017).

2017 Critical Raw Materials				
Antimony	Cobalt	Helium	Natural graphite	Phosphorus
Baryte	Fluorspar	HREEs	Natural Rubber	Scandium
Beryllium	Gallium	Indium	Niobium	Silicon metal
Bismuth	Germanium	LREEs	PGMs	Tantalum
Borate	Hafnium	Magnesium	Phosphate rock	Tungsten
				Vanadium

The chemical elements, which are now key components for the development of new technologies, are according to the present understanding of their concentrations, transformation and transport in the different environmental compartments, poorly studied (Reimann et al., 2010). This paper presents the GEMAS (Geochemical Mapping of Agricultural and grazing land Soil) results for Li, W and Sb, a project carried out by the Geochemistry Expert Group of EuroGeoSurveys in cooperation with Eurometaux (European Association of Metals). The GEMAS project aims were to detect and to map the element variation in productive soil at the European scale. Soil samples were collected from 33 European countries, covering an area of 5.6 million km^2 (Reimann et al., 2012a, 2014a, b). Reimann et al. (2016) argue for low sampling densities (1 site/100 to 1 site/18 000 km^2) rather than the costly and time-consuming very high sampling densities (100s–1000s of samples/km^2) employed for geochemical exploration, giving the same conclusions as those obtained in previous studies of geochemical mapping in continental- and regional-scale surveys (Smith and Reimann, 2008; Garrett et al., 2008; Cicchella et al., 2013; Birke et al., 2015). Reimann et al. (2007a, 2016) stated that this low-sampling density geochemical survey approach has also proved efficient in the early stages of mineral exploration programmes through identification of more suitable regions for detailed mineral exploration.

As part of GEMAS valorisation, a series of peer-reviewed publications, where detailed interpretation of the continental-scale distribution of single elements or related groups of elements, have been published, e.g., Reimann et al. (2012b - Pb); Ottesen et al. (2013 - Hg); Tarvainen et al. (2013 - As); Scheib (2012 - Nb); Sadeghi et al. (2013 - Ce, La, Y); Birke et al. (2014a, 2016, 2017 – Cd); Poňavič and Scheib (2014 – Se); Cichella et al. (2014 – U, Th, K); Ladenberger et al. (2015 - In); Albanese et al. (2015 - Cr, Ni, Co, Cu); Négrel et al. (2016 – Ge; 2018a – U, Th; 2018b - Rb, Ga, Cs); Jordan et al. (2018 – Ni). Among these publications, the elements In, Nb, Ge and the rare earth elements, although defined as technology-critical elements, have been interpreted in the frame of weathering patterns related to climate and inheritance from processes controlling element binding to mineral phases.

Even if we are not facing an imminent absolute shortage of energy critical elements (e.g., see the Hubbert's Peak scenario in Hubbert, 1982), market-driven shortages are possible, and no country can become independent from energy critical elements, which are nowadays produced often in politically unstable countries. Therefore, securing energy critical elements requires an advanced research plan including geological, metallurgical and materials science, the impact of which on knowledge and, therefore, the capacity to exploit resources is crucial for future development (Nickless et al., 2015; Ali et al., 2017). In this paper, we investigate the geochemical distribution and behaviour of three critical elements Sb, W and Li using low-sampling density geochemical mapping at the continental-scale and interpret the geochemical patterns in relation to their mineral potential. We need to point out the difference between a single mineralisation event, which cannot be located by using the GEMAS density of 1 sample/2500 km^2 and a mineralising process which affects a much larger area, a mineral province that can be identified with this data set (Bölviken et al., 1990). The GEMAS data set make it possible to define, therefore, potential areas, where follow-up and detailed geochemical exploration survey can be carried out in order to better define the mineralised zones (Reimann et al., 2007b).

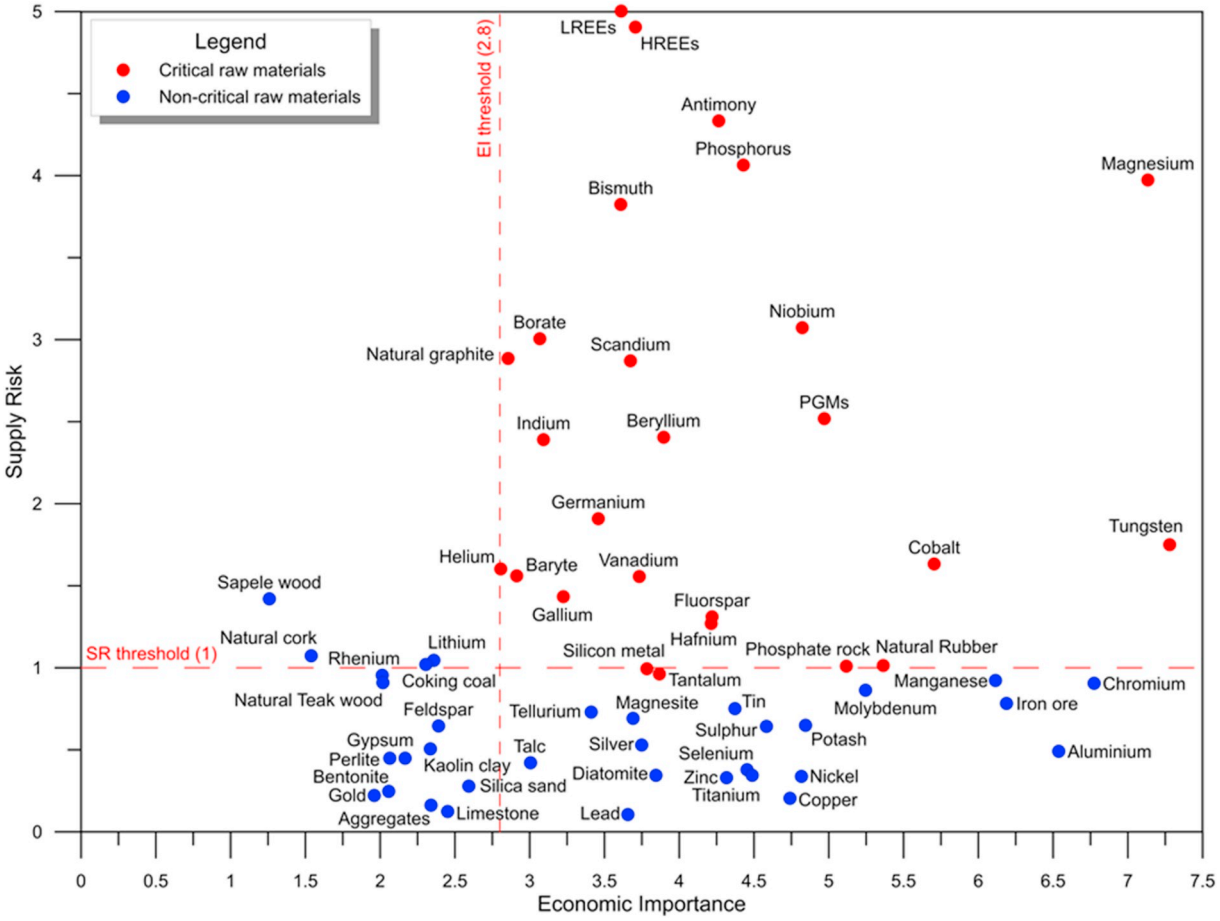

Fig. 1. Criticality assessment of economically important raw materials for the European Union in 2017 (redrawn from European Commission, 2017, Fig. 6, p.39).

2. Materials and methods

The GEMAS project (Reimann et al., 2014a, b) was carried out by the Geochemistry Expert Group of EuroGeoSurveys in cooperation with Eurometaux (European Association of Metals) and managed by the Geological Survey of Norway (NGU). It was the second large geochemical mapping survey at the European continental-scale following the FOREGS project (Salminen et al., 1998; Salminen et al., 2005; De Vos, Tarvainen et al., 2006). Agricultural and grazing land soil samples were collected in 33 European countries, covering an area of about 5.6 million km^2 (Reimann et al., 2012a, 2014a, b). The survey area is shown in Fig. 2. The main objective of the project was to detect and to map the element variation in agricultural and grazing land soil and to present their geochemical baseline variation for Europe. The soil samples were not taken at known contaminated sites, in the immediate vicinity of industry or power plants, cities, railway lines or major roads, directly below high power electric lines or near to pylons and wooden fences. The GEMAS aqua regia and XRF results are provided in a two-volume geochemical atlas (Reimann et al., 2014a, b).

For the GEMAS project two types of soil samples from two land use categories have been collected at an average density of 1 site per 2500 km^2 each (Fig. 2b). Grazing land soil (Gr; N = 2024 samples) has been defined as 'land under permanent grass cover' and a sample depth of 0–10 cm was used, according to the REACH regulation (Registration, Evaluation, Authorisation and Restriction of Chemicals) guidance document requirements (https://echa.europa.eu/). Agricultural soil (Ap; N = 2108 samples) was collected from the ploughing layer of an agricultural arable field from a depth of 0–20 cm. Each sample (ca 3.5 kg) corresponds to a composite of five sub-samples taken from the corners and centre of a 10 × 10 m square. Field duplicate samples were collected from both land use categories at a rate of 1 in 20 routine samples.

A single facility (State Geological Institute of Dionyz Stur, Slovakia) prepared all samples for analysis. Soil samples were air-dried, sieved to <2 mm using a nylon screen, homogenised and finally split into 10 subsamples. Two reference materials, e.g., standards, prepared in the same laboratory, were inserted at a rate of 1 in 20 samples together with field and analytical replicates to monitor analytical performance during the project. Samples were analysed by total X-ray fluorescence (XRF) and partial extraction methods like aqua regia (AR) and mobile metal ion (MMI®) (Reimann et al., 2012a, 2014a, b), and here the results of the AR method will be discussed.

The aqua regia extraction applied to the soil samples prior to analysis used a 15 g aliquot of the unmilled <2 mm fraction, which was leached in 90 ml of aqua regia (95 °C, 1 h) and then made up to a final volume of 300 ml with 5% HCl. The solutions were analysed using a combination of inductively coupled plasma-atomic emission spectrometry (ICP-AES) and inductively coupled plasma-mass spectrometry (ICP-MS) at ACME laboratories in Vancouver, Canada (now Bureau Veritas Mineral Laboratories). A total of 53 elements was determined on the over 5000 soil samples using matrix matched standards and reference materials.

A rigorous quality control (QC) procedure was part of the analytical protocol (Reimann et al., 2009; Demetriades et al., 2014). Samples were analysed in batches consisting of 20 samples (Reimann et al., 2009). In each batch, one field duplicate, one analytical replicate of the field duplicate and a project standard were inserted. The practical detection limit (PDL) was estimated from results of the project replicate samples by calculating regression line coefficients with the 'reduced major axis

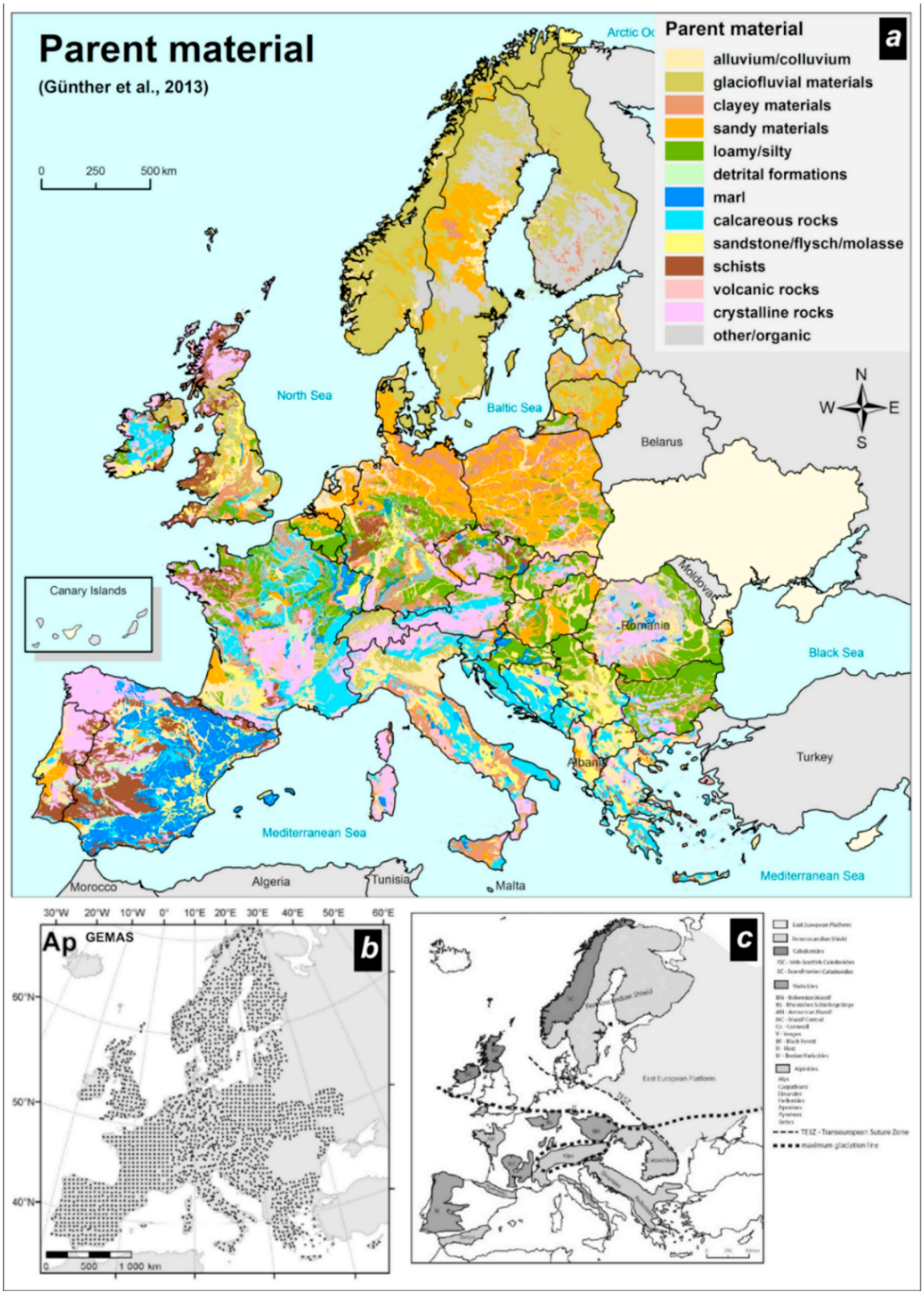

Fig. 2. Modified from Négrel et al. (2015, Fig. 1, p.3). (a) Map of parent materials in Europe showing the distribution of various lithologies across the continent (modified from Gunther et al., 2013 and adapted from Négrel et al., 2015, Fig. 1, p.3). (b) Sample locations (dots) of the ploughed agricultural soil (Ap-samples; N = 2108). Map projection: Lambert Azimuthal Equal Area (ETRS_1989_LAEA), with central meridian at 10°. (c) Generalised geological map of Europe with major lithotectonic units, Variscan and Alpine belts, Transeuropean Suture Zone (TESZ) and the extension of maximum glaciation (modified from Reimann et al., 2012b, Fig. 1, p.533).

line' procedure (Demetriades, 2011). This PDL in the aqua regia extraction by ICP-MS is 0.003 mg/kg for Sb, 0.01 mg/kg for W and 0.04 mg/kg for Li. Details on analytical procedures and quality control are provided in Reimann et al. (2009, 2011; 2012c), Birke et al. (2014b) and Demetriades et al. (2014).

Geochemical data are compositional data, element concentrations reported in wt % or mg/kg sum up to a constant and are thus not free to vary (Reimann et al., 2012d). Compositional data do not plot in the Euclidean space, but rather on the Aitchison simplex (Aitchison, 1986; Buccianti et al., 2006; Pawlowsky-Glahn and Buccianti, 2011). Thus, only order statistics should be used in statistical data processing. The colour surface maps were produced by kriging, based on a careful variogram analysis (Filzmoser et al., 2014). Kriging was used to interpolate values from the irregularly distributed sampling sites to a regular grid and into unsampled space. Class boundaries for the colour surface maps are based on percentiles (5, 25, 50, 75, 90 and 95). Geochemical maps displayed hereafter (Figs. 4–6) were produced in ArcGIS.

Table 2
Median values of Sb, W and Li (in mg/kg) from continental-scale geochemical surveys.

Provenance	Analytical information	Sb median (Sb range)	W median (W range)	Li median (Li range)	Source
World soil	<2 mm, total, estimate	1 (<0.2–10)	1.5 (0.5–83)	25 (3–350)	Bowen (1979)
FOREGS[a]-Atlas, EU, topsoil (0 - 25 cm)	<2 mm, total (ICP-MS[b], N = 845)	0.6 (<0.02–31.1)	<5.0[c] (<5.0–14)[c]	20.8 (0.28–271)[d]	Salminen et al. (2005)
GEMAS[e], EU, agricultural soil (0–20 cm)	<2 mm, AR[d] (ICP-MS[b], N = 2108)	0.23 (<0.02–17)	0.073 (<0.01–5.2)	11.4 (0.161–136)	Reimann et al. (2014a)
GEMAS, EU, agricultural soil (0–20 cm)	<2 mm, total XRF (N = 2108)	<5 (<0.5–36)	<5 (5–25)	n.d.	Reimann et al. (2014a)
GEMAS[e], EU, grazing land soil (0–10 cm)	<2 mm, AR[d] (ICP-MS[b], N = 2024)	0.28 (<0.02–25)	0.077 (<0.01–19)	11.3 (<0.1–153)	Reimann et al. (2014a)
GEMAS, EU, grazing land soil (0–10 cm)	<2 mm, total XRF (N = 2024)	<0.5 (<0.5–33)	<5 (<5–37)	n.d.	Reimann et al. (2014a)
USA, surface soil (0 - 5 cm)	<2 mm, total (ICP-MS[b], ICP-AES, N = 4857)	0.57 (<0.05–482)	0.8 (<0.1–1150)	20 (<1–300)	Smith et al. (2014)
USA, soil A-horizon	<2 mm, total (ICP-MS[b], ICP-AES[f], N = 4857)	0.57 (<0.05–630)	0.8 (<0.1–299)	20 (<1–514)	Smith et al. (2014)
Australia, NGSA[g], TOS[h] (0 - 10 cm)	<2 mm, AR[d] (ICP-MS[b], N = 1190)	0.12 (<0.02–18.1)	N/A[i] (<0.1–174)	N/A[i]	Caritat and Cooper (2011a, b)
Australia, NGSA[g], TOS[h] (0 - 10 cm)	<0.075 mm, AR[d] (ICP-MS[b], N = 1177)	0.15 (<0.02–27.1)	N/A[i] (<0.1 – >200)	N/A[i]	Caritat and Cooper (2011a, b)
Australia, NGSA[g], TOS[m] (0 - 10 cm)	<0.075 mm, HF + HNO_3 (ICP-MS[b], N = 1187)	N/A[i] (<0.4–28.9)	1.6 (<0.1–643)	N/A[i]	Caritat and Cooper (2011a, b)
Australia, NGSA[g], TOS[m] (0 - 10 cm)	<2 mm, HF + HNO_3 (ICP-MS[b], N = 1190)	N/A[i] (<0.4–14.5)	1 (<0.1–327)	N/A[i]	Caritat and Cooper (2011a, b)
China, RGNRP[j], silt or fine sand on the drainage bottom, bank soil or dry stream sediment	<0.22 mm, total, (N = 1,568,528)	0.6 (<0.03–911)[k]	1.71 (<0.04–1073)[l]	31.1 (<0.4–560)	Xie et al. (2012)
BSS[n], agricultural soil (0 - 25 cm)	<2 mm, HF (ICP-MS[b], N = 747)	0.24 (<0.1–3.2)	N/A[i]	N/A[i]	Reimann et al. (2003)

[a] FOREGS - Forum of European Geological Surveys.
[b] ICP-MS - Inductively Coupled Plasma Mass Spectrometry.
[c] XRF - X-ray Fluorescence Spectrometry.
[d] Stream sediment.
[e] GEMAS - Geochemical Mapping of Agricultural and Grazing Land Soil in Europe.
[f] ICP-AES - Inductively Coupled Plasma Atomic Emission Spectrometry.
[g] NGSA – National Geochemical Survey of Australia.
[h] TOS - top outlet sediment.
[i] N/A – not available/applicable.
[j] RGNRP – Regional Geochemistry National Reconnaissance Programme.
[k] HG-AFS – Hydride Generation-Non-Dispersions Atomic Fluorescence Spectrometry.
[l] POL – Polarography.
[m] GF-AAS - Graphite Furnace Atomic Absorption Spectrometry.
[n] BSS - Baltic Soil Survey: Agricultural Soils in Northern Europe. A Geochemical Atlas.

Table 3
Explanation of Sb anomalies in Europe: comparison with ProMine Mineral Database (PMD; Cassard et al., 2012, 2015). For anomaly numbers see Fig. 4a.

No.	Country	Explanation (PMD)	Other explanation
1	Sweden (N Sweden)	Various sulphide deposits with Zn, Ag, Au, Cu, Pb	Skellefte Ore District
2	Sweden Central Sweden)	Zn–Cu–Pb deposits	Black shale in the Lower Allochthon in the Caledonides
3	Sweden (SE Sweden)	Associated with Zn–Pb and W mineralisation (associated with Mo and Sb)	
4	Norway (S Norway)	Sulphide mineralisation in volcanic rocks of the Oslo Rift, Cu–Mo and Au deposits	
5	Finland (S Finland)	Au deposits associated with Ag, Cu, Bi and Sb	
6	Denmark, (E Jutland)	Fe mineralisation in young postglacial sediments	
7	Poland (central-northern Poland)	Lignite deposits (Miocene) or sedimentary Fe deposits (Jurassic)	
8	SW Poland/SE Germany	Lignite deposits (active opencast mines)	Former lignite power plants and ash dumps, old opencast lignite mines
9	Ukraine	Hg deposits associated with silicified sandstone and coal (Donbass region	
10	United Kingdom (Scotland)	Various sulphide mineralisation with Sb, associated with Cu, Mo, Au and Ag; Coalfield region.	
11	United Kingdom (Bradford-Manchester)	Old mining region with Pb deposits, sphalerite, pyrite, galena, chalcopyrite, F and Ba. Coalfield region	
12	United Kingdom (Cornwall)	Sb sulphide mineralisation, associated also with Pb, W and Sn. Fault-related vein deposits	
13	Eastern Ireland	Sulphide deposits with Zn, Au, Cu, Pb and Sb, e.g., in Glendalough, Wicklow and Avoca region)	Possible contribution of contamination from the capital city of Dublin
14	Netherlands (Amsterdam)		Anthropogenic anomaly related to Amsterdam city
15	Germany (Rhenish Slate Mts, Nordrhein-Westfalen, Rheinland-Pfalz	Sb sulphide deposits, limonite occurrences and historical smelting	Pb–Zn-(Ag) sulphide deposits in the Stolberger mining district
16	Central Germany (Mansfeld, Lutherstadt Eisleben, Gräfenroda)	Northern anomaly: Cu Kupferschiefer deposits; Pb smelter	Southern anomaly: Thuringian Forest, Cu–Pb–Zn–Ag mineralisation following the Hercynian Eichenberg-Gotha-Saalfelder fault zone; Copper shale deposits (abandoned Cu mines and mining heaps)
17	Germany (Erzgebirge, East Thuringian Slate Mts)	Polymetallic vein mineralisation Bi–Co–Ni–Ag–U, arsenides	Eastern Ore Mts.: Sn deposits, Altenberger ore district, Schellerhauer granite; Western Ore Mts.: Kirchberger granite, W–Mo mineralisation, hard coal deposits near Oelsnitz; Sb-(Ag–Pb–Fe–As) mineralisations in the Berga Antiform
18	SW Germany (Karlsruhe-Stuttgart region; Pforzheim in Schwarzwald)	Open pit mining with fluorite associated by Bi and Cu in vein and breccia deposits	
19	S Germany - W Austria (Insbruck region)	Leogang (inactive plant) with Fe, Mn, Co, Ag, Cd, Hg, Ga, In, Ge, Sn, Sb	
20	Czech Republic (Plzen)	Coal and lignite deposits with Ge (Plzen and Radnice basin); Sb (antimonite)-Zn-Pb deposits	
21	Czech Republic/Poland	Fe deposits with Sb; coal deposits	
22	Czech Republic (Opava)	Pb mineralisation; minor coal deposits	
23	Central Slovakia	Numerous Sb deposits (with Sb, Pb, Zn, Ag and Au)	Few localities with larger findings of Sb minerals, together with Au and Ag in hydrothermally altered Miocene andesites - www.mindat.org)
24	Hungary (N of Budapest, Visegrad)	Pb–Zn mineralisation	Anthropogenic anomaly – Budapest City
25	E Austria/W Hungary	Sb–Hg mineralisation; lignite deposits	
26	S Austria	Carbonate-hosted Pb–Zn deposits (MVT) with Ga, Ge, Pb, Zn; Cu VMS deposits; inactive plants (mainly surface storage)	
27	W Austria (Insbruck)	Pb–Zn deposits; skarn deposits with W; Cu deposits; inactive plants (mainly surface storage)	
28	W Austria/N Italy	Minor Zn mineralisation (with Ga and In); inactive plants (mainly surface storage)	
29	Slovenia	Sb mineralisation (vein and disseminated); Pb–Zn carbonate-hosted deposits (MVT)	
30	Bosnia & Herzegovina (Sarajevo region)	Sb mineralisation; Pb–Zn mineralisation; open pit mining (Pb–Zn with Sb)	
31	Serbia	Cu–Au VMS deposits; Sb vein deposit; Sediment-hosted precious metal deposits	
32	S Serbia	Sediment-hosted precious metal deposits with Sb; Pb–Zn Sedex deposits; coal deposits	
33	SE Serbia/North Macedonia	Sb deposits; Pb–Zn + Ag skarn mineralisation; Sb deposits with stibnite	
34	N Cyprus		Western part of the Kyrenia Terrain (Alpine orogenic belt); however, it is most likely a transported anomaly, and related to the Troodos Ophiolite complex massive sulphide mineralisation; it correlates with anomalous Ag, Au, As, Hg, Pb, S, V and Zn
35	Central Italy	Sb deposits	
36	Central Italy	Sediment-hosted Sb mineralisation, related to shallow intrusions	Rome – anthropogenic anomaly; young volcanic rocks in the Rome region
37	S Italy (Naples)		Naples anthropogenic anomaly; young volcanic rocks (Vesuvius) which are responsible for Sb enrichment in local soil and groundwater
38	SE Sardinia (Italy)		

(*continued on next page*)

Table 3 (*continued*)

No.	Country	Explanation (PMD)	Other explanation
		VMS deposit with Sb (antimonite); Pb–Zn deposits, Ag–Sb mineralisation, Zn–Sb carbonate-hosted stratabound and vein mineralisation (MVT)	
39	E France	anthropogenic	Verdun – WW1
40	E France (Vosges)	Sb mineralisation; Pb–Cu–Ag mineralisation	Similar anomaly is observed for Pb (Reimann et al., 2012b); Variscan orogen
41	N France	Sediment-hosted baryte-Sb deposits, vein and metasomatic polymetallic deposits with Sb, Cu, Pb	
42	NW France	Polymetallic, mainly vein types deposits with Sb, Bi, Mo, Sn, W in granitic host rocks	
43	W France	Carbonate-hosted (in karst) Pb–Zn (+Ag) deposits MVT, known since medieval time; historical Ag smelting	
44	France (Limoges, Haute-Vienne, W Massif Central)	Carbonate-hosted Pb–Zn (Ag) MVT deposits; several Sb mineralisation with stibnite and berthierine, related to numerous Au deposits	Au-bearing granitic mica schist
45	France (S Massif Central)	Pb–Zn (Ag) deposits; Sb mineralisation with stibnite, a large system of Au and sulphide-rich quartz veins	
46	France (Massif Central, S of Clermont Ferrand, and west of Lyon)	Numerous Sb mineralisation associated with Au, Ag, Pb, Zn; mainly fault-related	
47	SE France (Grenoble)	Cu–Pb–Ag + Au (±Sb) fault related deposits, sandstone ± dolomite hosted Pb–Zn + Ag + Sb deposits	
48	NE Spain/Andorra (Pyrenes)	Volcano-sedimentary Zn–Ag deposits	
49	NE Spain (S Pyrenes)		Various polymetallic mineralisation (Pb–Zn–Cu–Ag–Sb–Bi–As–W–Au) in the pre-Pyrenean and Pyrenean region (Locutura et al., 2012)
50	S coast of Spain (Granada region)	Fault-related vein and breccia deposits with Ag, Zn (galena); vein and disseminated Sb deposit; carbonate-hosted Pb–Zn deposits with Ag	
51	Central Spain	Sb vein deposits; fault-related Pb–Zn–Ag deposits	
52	Central Spain (N of Cordoba)	Pb–Zn–Ag deposits (with galena, sphalerite)	
53	SW Spain	Iberian Pyrite Belt: Zn–Pb–Cu (+Ag) VMS deposits	
54	NW Spain (Galicia, Oviedo region)	Coal deposits; numerous Au deposits (quartz veins, conglomerate and alluvial placer); Sb (stibnite) deposits with cinnabar	
55	NE Portugal	Au–As mesothermal deposits (Au, Ag, As, Zn, Pb); Sn–W deposits (cassiterite, wolframite, scheelite, silver, pyrite, arsenopyrite, marcasite) in granitic veins and stockworks (greisen)	
56	Central Portugal	Sb–W fault-related deposits; Au–Sb mineralisation	
57	S Portugal	Sb fault-related deposits (antimonite, malachite, baryte, silver); Zn–Pb–Cu (+Ag) VMS deposits	

3. Results and discussion

3.1. Element concentrations in agricultural soil

The concentrations of Sb, W and Li generated by the GEMAS project constitute a homogeneous data set and can be compared, but are not compatible, with other continental data sets, e.g., from Europe (FOREGS; Salminen et al., 2005; De Vos, Tarvainen et al., 2006), U.S.A. (Smith et al., 2013, 2014), Australia (Caritat and Cooper (2011a, b, c, d) and China (Xie et al., 2012) as tabulated in Table 2.

3.1.1. Sb concentrations in agricultural soil

The median for Sb in the Ap and Gr soil samples in Europe in the hot aqua regia extraction are very close, 0.234 and 0.275 mg/kg, respectively. The combined plot histogram - density trace one - dimensional scattergram - boxplot shows the univariate Sb data distribution (Fig. 3a for Ap, and 3b for Gr samples). The existence of outliers in the Sb distribution is shown by one-dimensional scattergram and boxplot. The density trace displays a smooth multimodal distribution, but is overall symmetrical about the median, a feature also indicated by the very symmetrical boxplot (log-scale). Compared to the upper continental crust (UCC) estimated Sb abundance of 0.4 mg/kg (Hu and Gao, 2008), the aqua regia extractable Sb (median Ap 0.234 and Gr 0.275 mg/kg) is lower by a factor of 1.74 in the Ap samples, and 1.45 in the Gr soil samples. Due to high detection limits of GEMAS XRF results, it is not possible to directly relate GEMAS total concentrations to the UCC values. However, estimated extractability of Sb (from the comparison of aqua regia and XRF results) is 9 and 13% for the Ap and Gr samples, respectively (Reimann et al., 2011).

An explanation for the difference between UCC (total concentrations) and hot aqua regia results is that a major quantity of Sb occurs in minerals and phases which are not easily dissolved by acids. Sulphides, major host minerals for Sb, may not be very common in average soil. On the other hand, Sb can sorb onto Fe, Mn and Al oxides and hydroxides, clay minerals, and organic matter (Belzile et al., 2001; Buschmann and Sigg, 2004; Johnson et al., 2005), especially, when it occurs as oxy-anions in low pH environments (Takahashi et al., 2010; Hockmann and Schulin, 2013). Some of the Sb can also be volatilised and lost during the hot acid extraction (Reimann et al., 2010).

The median Sb values and their concentration ranges in soil samples of different continental-scale surveys are provided in Table 2. The median Sb values vary between 0.12 mg/kg in Australia and 0.6 mg/kg in the European FOREGS topsoil. The Sb 'world soil' median of 1 mg/kg (with a range from <0.2 to 100 mg/kg), as provided by Bowen (1979), is about four times higher than the GEMAS hot aqua regia extractable Sb median. Kabata-Pendias and Mukherjee (2007) provide better-constrained Sb concentrations with the background level of Sb in topsoil samples between 0.05 and 4.0 mg/kg. Recently, the Sb data set of the LUCAS Soil Survey (AR; ICP-AES; N = 23,000; Cristache et al., 2014; ECS, 2010) published by Tóth et al. (2016) reports values from 0.01 to 10.9 mg/kg with a calculated mean of 0.25 mg/kg. The GEMAS median values for agricultural and grazing land soil samples (Reimann et al., 2014a, b), based on 2108 samples, are thus comparable to those reported by the LUCAS project based on over 23,000 samples. An advantage of the GEMAS results is that they are based on two separately analysed and statistically treated land-use sample types (Ap and Gr)

Table 4
Explanation of W anomalies in Europe: comparison with ProMine Mineral Database (PMD; Cassard et al., 2012, 2015). For anomaly numbers see Fig. 5.

No.	Country	Explanation (PMD)	Other explanation
1	N Sweden	Cu–Ag mineralisation with scheelite occurrences	W mineralisation in skarn; associated Cu, Zn, Au, Ag mineralisation (SGU database)
2	Central Sweden	Au–Cu + Ag mineralisation	Many small W mineralised occurrences and historical W (+Pb + Cu) mining (SGU database)
3	Central Sweden (Bergslagen)	Scheelite mineralisation (+Mo, Fe–Cu–Ag) and historical mining sites	
4	W Norway (Molde-Ålesund)		Mineralisation in quartz-rich lithologies, V–Fe–Ti mineralisation in western Norway (FODD database)
5	S Norway (Bergen, Odda)		Small granitic intrusions, Zn–Cu–Au mineralisation (source: FODD database); Odda - a major Zn smelter in Norway
6	Central Finland	Mineralisation in pegmatites, numerous gold occurrences	
7	S Finland	Scheelite-Mo (As + Co) skarn mineralisation, associated Au mineralisation	
8	SW Ukraine		Epithermal polymetallic deposits in Transcarpathian region. Vein-type Au-base metal deposits hosted by volcano-sedimentary sequences of the Pannonian basin in the Carpathian Neogene volcanic belt
9	SW Ukraine		Au–Ag–Zn–Pb–Cu mineralisation and epithermal deposits in Transcarpathian region
10	Scotland	Wolframite-scheelite mineralisation in Devonian granites (associated with cassiterite, molybdenite, sphalerite, chalcopyrite, topaz)	
11	Scotland W (Southern Uplands)	Au–Pb–Cu–As–Ag mineralisation	
12	NW England (southern part of Lake District and Pennines)		W mineralisation in the Lake District (Cumbria)
13	United Kingdom (SE Wales, Cornwall)	Wolframite-cassiterite mineralisation (Cs + Li) in Cornubian orefield	W mineralisation in Cornubian batholith
14	NE Netherlands	unexplained	
15	NW Germany (Lower Saxony)	Fe–Ag–Pb–Zn mineralisation in felsic alkaline plutonic rocks; metasomatic carbonate-hosted haematite-magnesite deposits; Fe smelter	Abandoned iron ore mines
16	W Germany (North Rhine-Westphalia)	Fe smelter	Hard coal deposits and mining, inactive hard coal power plants
17	Rhineland-Palatinate	Minor Ag–Cu mineralisation	Donnersberg rhyolite massif, historical Cu mines
18	Central Germany (Thuringian Forest)	Cu–Pb–Zn–Ag mineralisations	Cu–Pb–Zn–Ag vein mineralisation following the Hercynian Eichenberg-Gotha-Saalfeld fault zone; Cu shale deposit
19	SE Germany (Erzgebirge, Ore Mts)	Sn–W (+Ag + Zn + Ge) mineralisation in greisen	W–Mo mineralisation in the area of Kirchberger granite
20	S Germany (W and NE Nürnberg)/W Czech Republic	U–W (+Sn) mineralisation	Pb–Zn mineralisation, Baryte-fluorspar-haematite mineralisation
21	S Germany (Molasse basin)	Minor Pb–Zn mineralisation	Pitch coal occurrences (strong pressed lignite) in the south
22	Central Czech Republic	W and Pb–Ag mineralisation	
23	SW Slovakia-NW Hungary	Au–Sb–Ag–Zn–Pb mineralisation	
24	SW Bulgaria (Western Rhodopes Mts)	polymetallic W–Bi–Mo deposits; W–Pb–Mo–Cu mineralisation in granite and skarn	
25	Hellas (Central Macedonia)	Sb–W vein mineralisation; Cu–Ag–Au porphyry deposits	
26	W Austria (Insbruck, Hohe Tauern)	Numerous W occurrences (scheelite-Mo skarn)	
27	S Switzerland	Au, REE, Pb–Ag–Zn mineralisation	
28	N Italy	Zn–Ag carbonate-hosted mineralisation	
29	NW Italy	Cu–Ag mineralisation	
30	Central Italy	Minor Sb (Hg, Cu, Zn, Pb) mineralisation	Volcanic origin
31	Central Italy (Rome-Naples region)		Volcanic origin
32	Italy (Gargano Peninsula)		Plutonic and volcanic alkaline rocks (gabbro and syenite, anorogenic lamprophyres); skarn mineralisation at the contact with limestone
33	SE Sardinia	W–Zn–Pb mineralisation; Mo–W mineralisation in greisen; Sb–W VMS deposits; Au mineralisation; Ag–Sb–Pb–Zn polymetallic veins	
34	N France	unexplained	
35	NW France	W (scheelite) – Mo skarn mineralisation; wolframite in greisen	
36	W central France (Poitu, Limousin, Haute-Vienne)	Numerous W (+Mo, Sn, Zn, Cu) mineralised occurrences in relation to granitic intrusions and in greisen	
37	Central France	W (+Sn, Mo, Py) mineralisation in granite and greisen	
38	E France (Vosges)	Numerous W mineralisation; W–Mo skarn; wolframite and scheelite in greisen	
39	Central France (Massif Central)	Numerous W mineralisation (+Bi, Sn, As, Mo, Cu)	
40	S France (Provence-Alpes-Côte d'Azur region)	Numerous W mineralisation, carbonate hosted Pb–Zn MVT deposits; W–Mo skarn deposits in greisen (with Sn)	

(*continued on next page*)

Table 4 (*continued*)

No.	Country	Explanation (PMD)	Other explanation
41	S France (Pyrenees)	W–Mo skarn mineralisation, associated with Au and Ag	
42	S France (Pyrenees)	W–Mo skarn mineralisation, associated with Ag, Zn and Pb	
43	N Spain	Minor Ag occurrences	
44	Central Spain, near Madrid	W–Mo in skarn; W–Sn mineralisations	
45	W Spain	W mineralisation	
46	S central Spain (Cordoba)	W mineralisation (with associated As, Ag, tourmaline)	
47	NW Spain (Galicia)	W–Fe–Sn mineralisation	
48	NW Spain (Galicia)	Au and W mineralisations in granite-greisen-quartz veins	
49	N Portugal	W mineralisation in pegmatites (scheelite, wolframite); W–Sn mineralisation with associated Au (Ag)	
50	N Portugal	W–Sn–Cu–Zn mineralisation in granite and greisen	

evenly covering the whole survey area, while in the LUCAS project various land-use materials were analysed and processed together. None of these different land-use classes provided an even coverage of the European continent.

Some European regional geochemical surveys also provide Sb background data. In the Baltic Soil Survey (Reimann et al., 2003), the median Sb concentration (HF extraction) is 0.24 mg/kg in TOP (0-25 cm) soil, which is nearly identical with the GEMAS median and its concentration ranges between <0.1 and 3.2 mg/kg, while in the BOTtom (50-75 cm) soil it is lower, 0.19 mg/kg (range: <0.1–1.41 mg/kg). The total Sb concentrations in topsoil samples (0–15 cm) of England and Wales (Rawlins et al., 2012) range from 0.1 to 55 mg/kg, with a median value of 0.7 mg/kg. In Irish topsoil (0–10 cm), the median value of Sb is 0.53 mg/kg and the total concentrations vary from <0.05 to 5.29 mg/kg (Fay et al., 2007).

3.1.2. W concentrations in agricultural soil

The median concentration of extractable W (aqua regia extraction) in the GEMAS European soil is 0.073 mg/kg in the Ap and 0.077 mg/kg in the Gr samples. The combined plot histogram - density trace one-dimensional scattergram - boxplot shows the univariate data distribution of the aqua regia extractable W (Fig. 3c for Ap and 3d for Gr samples). The one-dimensional scattergram and boxplot display the existence of upper and lower outliers in the W distribution. The density trace, histogram and one-dimensional scattergram highlight the samples below detection. The main body of the density trace and histogram exhibit an almost symmetrical data distribution in the log-scale.

Because W does not substitute into most rock-forming minerals, its distribution in soil is related largely to naturally occurring W mineralisation. Tungsten is enriched in mica (5–50 mg/kg), and muscovite in altered granite near W deposits may contain up to 500 mg/kg (Wedepohl, 1978). A comparison of the GEMAS Ap soil W median to the upper continental crust (UCC) estimated abundance of 1.9 mg/kg (Hu and Gao, 2008) shows that the hot aqua regia extractable W is a factor of 27 lower in the European agricultural soil. Clearly, only a very small percentage of total W in soil can be extracted by the mixture of HCl and HNO_3, even after heating. XRF results for W in the GEMAS project vary around the method's detection limit, but the interpretation of the data range and its maximum values indicates that the data set is quite homogeneous, without many outliers. The extractability of W from the comparison of aqua regia to XRF results is 3 and 4% for the Ap and Gr samples, respectively (Reimann et al., 2011). The AR extraction is, therefore, not a sufficiently good method for extracting W from soil samples, mainly because of the presence of resistant W-bearing minerals and precipitation of insoluble tungstates and the polymerisation of tungstates onto soil particles (Bednar et al., 2010).

Apart from the GEMAS project XRF results for W (Ap samples: <5–25 mg/kg, with a median of <5 mg/kg; Gr samples: <5–37 mg/kg, with a median of <0.5 mg/kg), total W concentrations, have been reported in three continental-scale soil geochemical projects, i.e., the Geochemical Atlas of Europe (FOREGS; Salminen et al., 2005), the Geochemical and Mineralogical Atlas of the Conterminous United States; Smith et al., 2014), and the Geochemical Atlas of Australia (Caritat and Cooper, 2011a,b), all ranges and medians are tabulated in Table 1. In the United States of America, the areas of very high total W values in the Central and Southern Rocky Mountains are related to the Colorado Mineral Belt and the Butte Mineral district in Montana (Smith et al., 2014). Mineral deposits enriched in W are widespread throughout the western United States and are most often genetically related to intrusions of felsic rocks.

In Europe, total W contents in the topsoil of England and Wales vary at the regional scale from <0.6 to 70 mg/kg, with a median of 2.1 mg/kg (Rawlins et al., 2012). The anomalous W concentrations in southern Devon and Cornwall are associated with mining and extraction processes and occur around the granite intrusions of Dartmoor, Bodmin Moor and St. Austell. In the Soil Geochemical Atlas of Ireland, W concentrations range between <0.1 and 7.72 mg/kg, with a median of 0.59 mg/kg (Fay et al., 2007). High and elevated levels of total W are found in soil developed on igneous rocks as well as on greywacke, black shale and fine-grained sandstone (Fay et al., 2007).

3.1.3. Li concentrations in agricultural soil

The median concentration of Li in an aqua regia extraction in the GEMAS European soil is 11.4 mg/kg in Ap and 11.3 mg/kg in Gr samples. The combined plot histogram - density trace one - dimensional scattergram - boxplot displays the Li univariate data distribution in Ap and Gr soil samples (Fig. 3e for Ap and 3f for Gr samples). One-dimensional scattergram and boxplot highlight the existence of many outliers at the lower end of the Li distribution and very few at the upper end. Though the density trace, histogram and boxplot suggest a slight skew, the data distribution is still rather symmetrical in the log-scale, for both Ap and Gr types of soil. During weathering processes, water-rock interaction and erosion, the geochemical behaviour of Li is similar to that of Na, despite the difference in the abundance of both elements. However, Li is more mobile in the surficial environment and during water–rock interactions. Owing to its weaker binding than Na in ion exchange reactions, Li is preferentially leached during weathering of silicate rocks. Lithium is very mobile during hypergenetic processes, as well as in the initial stage of soil formation (Kabata-Pendias and Mukherjee, 2007). It may become more stable due to its adsorption to clay minerals, Fe and Mn hydroxides, and organic matter (Millot et al., 2010).

The comparison of Li to the estimated upper continental crust (UCC) abundance of 24 mg/kg (Hu and Gao, 2008) shows that the hot aqua regia extractable Li is almost a factor of 2 lower in the European agricultural soil samples. Large differences in the median values of Li in GEMAS and in continental-scale geochemical soil surveys (Table 2) from China, U.S.A. and Australia indicate that natural factors such as underlying geology, and technical aspects like number of samples, sample size and methodology play a crucial role in data processing and interpretation.

Table 5
Explanation of Li anomalies in Europe: comparison with ProMine Mineral Database (PMD; Cassard et al., 2012, 2015). For anomaly numbers see Fig. 6.

No.	Country	Explanation (PMD)	Other explanation
1	E Sweden		Occurrences of LCT (Lithium-Cesium-Tantalum) pegmatites of the Varuträsk type
2	Central Sweden		Li (Sn, Ta) mineralisation (FODD database); Sn, Li, Nb, Be, Ta occurrences (SGU database)
3	Central Sweden (Bergslagen)	Li in pegmatites (spodumene, beryl, cassiterite); Li–Fe in magnetite skarn; REE and pegmatite occurrences	Lithium seems to be enriched in some Fe deposits
4	Norway (Oslo Rift)		Mineralisation in pegmatites; Mo mineralisation
5	S Finland	Ta, Be, Li, Sn in pegmatites	Rapakivi granites; Li mineralisation
6	S Finland		Rapakivi granite
7	SE Poland	unexplained	
8	SW Ukraine (Carpathians)	unexplained	
9	E Ukraine (Donetsk region)	Li mineralisation	Phosphate-Be-REE-Ta-Nb deposits; Li deposits in eastern Ukraine (petalite and spodumene in pegmatites)
10	United Kingdom (Wales)		Li-bearing secondary manganese minerals in hydrothermal ore deposits and sedimentary Mn deposits
11	United Kingdom (Cornwall)	Li and Cs in pegmatites and aplites (Li, Ta, Nb, Be)	Cornubian batholith (lithium-mica-albite-topaz granites)
12	SE Ireland (Wexford)	Li mineralisation in pegmatites; LCT pegmatites (Lithium-Cesium-Tantalum)	
13	W Germany (Northern Hesse, Sauerland, SE Dortmund)	Unexplained; coal?	Slate mining (roof slate); fluorspar and baryte mining; hard coal power plant in the region; industrial region with different types of industry (metalworking) and steel production
14	W Germany (Rhenish Slate Mts., SE Bonn)	Kaolin occurrences; phosphorites	
15	SW Germany (Saarland)	Oolitic Fe-ores; Cu–Pb–Zn mineralisation	Hard coal deposits, former hard coal power plants and iron and steel works
16	SW Germany (Central Black Forest)	Au-Ge-Ag, galena, fluorspar occurrences	Pb–Cu–Fe and Fe mineralisation, Triberger biotite granite
17	SE Germany/W Czech Republic (West Erzgebirge, Western Ore Mts.)	Numerous Li occurrences in LCT pegmatites	Li in Sn mineralisation (cassiterite-quartz association) and in Li-bearing micas in granites
18	S Czech Republic	unexplained	
19	S Austria	Li mineralisation in LCT pegmatites	
20	W Austria (Insbruck)/N Italy	Li mineralisation in LCT pegmatites	
21	E Slovenia	unexplained	
22	SE Croatia/S Bosnia & Herzegovina/Montenegro	Fe deposits (oolitic iron deposits); bauxite deposits in karst and laterite; inactive Al plant	Karst/bauxite weathering
23	W Bulgaria	Granite-controlled Au–Cu deposits with quartz veins; supergene clay deposits	
24	NW Hellas (Epirus)	Laterite related polymetallic deposits (Ni, As, Au, Co, Cr, Fe, Mg, Mn, Pd, Pt); Ophiolite related VMS deposits (Cu, Zn, Co)	Karst/bauxite weathering; correlation to mafic and ultramafic rocks (ophiolite) and Fe–Ni deposits; phosphorites; evaporites (by the coast)
25	C Hellas (Sterea Elladha)	Bauxite and Al-rich rocks deposits (in karst and laterite); mine waste dump with 'red muds' from bauxite refining	Karst/bauxite weathering? Possible correlation to mafic and ultramafic rocks and Fe–Ni deposits
26	SE Switzerland	Ta–U mineralisation in felsic alkaline rocks	Mineralisations in quartz veins, pegmatites
27	NW Italy (Genoa, Portofino)	Volcano-sedimentary Mn mineralisation with jasper and chert; Cr mineralisation in mafic-ultramafic rocks (Cu–Zn, Co VMS deposit)	
28	Central Italy (Ravenna)		Valli di Comacchio: brackish lagoons with brines which might be enriched in lithium
29	Central Italy (including island of Elba)	Li – Cs - REE mineralisation in pegmatites; Sb (+Hg) mineralisation	Related to the igneous rocks from Roman Alkaline Province
30	Italy	unexplained	
31	Italy (Gargano Peninsula)	Bauxite deposits and Al-rich rocks in karst/laterite	Possibly related to the plutonic and volcanic alkaline rocks (gabbro and syenite, anorogenic lamprophyres
32	Italy (Southern Apennines)	unexplained	
33	N Corsica (France)	Granitic-pegmatitic veins and greisens (W–Mo, Ag)	
34	S Belgium (Dinant, Ardennes)	Vein deposits with fluorspar, baryte, sphalerite, galena, etc; historical mining	Kaolinised regoliths
35	NW France (Hercynian Armorican Massif)	Peraluminous leucogranites, pegmatites and peri-granitic veins (associated with U, Sn, W, REE, Zr and beryl)	
36	NW France (Poitu)	Associated with W-baryte-kyanite deposits, carbonate-hosted veins with Ba and F deposits (MVT)	
37	S Central France (Massif Central)	Li mineralisation in pegmatites associated with beryl, cassiterite, Ta–Nb, Y and REE; numerous occurrences with Sn, W, Au, Ag	
38	S Central France (Massif Central)	Numerous occurrences (+Sn, As, Fe, W, Ag, Au) in granitic and peri-granitic veins and in greisens	
39	SE France (Grenoble)	Cu–Sn–Ag–Mo–Bi and baryte-fluorspar granite-controlled mineralisation; In–Zn, fluorspar mineralisation, fault-related; granitic and peri-granitic veins; historical mining	
40	S France/N Spain (Pyrenees)	W–Mo skarn mineralisation, associated with baryte; Ag, Zn and Pb; Zn–Ag, Co–Sn Pb (+Ga, Ge) mineralisation; historical mining	
41	N Spain (Zaragoza)	Clays and evaporitic salts deposits	This anomaly in south Pyrenean Zone correlates well with Li anomaly (partial extraction) in sediments in Geochemical Atlas of Spain (Locutura et al., 2012).
42	Central Spain (Madrid)		

(*continued on next page*)

Table 5 (*continued*)

No.	Country	Explanation (PMD)	Other explanation
		Sn, W, Ag mineralisation related to granite, pegmatite, greisen and quartz- and mica-rich (muscovite) veins; W–Mo skarn mineralisation	
43	S Central Spain	W, Sn, quartz, tourmaline; As, Fe, Ag, Au, Pb mineralisation in granite-pegmatite rocks	Related to Iberian Massif (Central Iberian Zone); the Almadén mercury mining district
44	NW Spain (Galicia)	Associated Au–As mineralisation in quartz-rich veins; Fe–Sn–W–Cu in granites and pegmatites	Hercynian granite; Li-rich mineral occurrences associated with aplite-pegmatite dykes and sills intruded in granitic and metasedimentary rocks of Galicia – Trás-os-Montes geotectonic zones
45	NW Spain (Galicia)	Associated with Au–Ag in quartz-rich veins; Sn–Ta–Nb, quartz, kaolin and REE mineralisation	Hercynian granite
46	N Portugal (Braga)	Lepidolite, spodumene, petalite mineralisation in pegmatite, associated with W–Sn–Au–Ta vein mineralisation zone	Galicia - Trás-os-Montes Zone; aplite-pegmatite veins in a late Hercynian granite, rich in spodumene, embedded in Silurian metasediments
47	Central Portugal (Castelo Branco)	Li mineralisation in aplites and pegmatites, associated with W–Sn–Au, Ta–Nb, ilmenite, beryl mineralisation	The Central-Iberian Zone; aplite-pegmatite veins in a late Hercynian granite

3.2. Spatial distribution of Sb, W and Li in European soil and their source geology

As very few differences are observed for the three elements between Ap (ploughing layer of agricultural arable fields) and Gr (land under permanent grass cover) types of soil only the data obtained for the Ap soil samples will be considered hereafter.

At first glance, geochemical maps for Sb, W and Li (Figs. 4b, 5b and 6b) reflect natural sources of these elements and their spatial distribution seems to be governed by weathering type and degree, Quaternary history, the underlying bedrock and mineralisation. The chemical composition of soil represents largely the primary mineralogy of the source parent materials, the effects of pre- and post-depositional chemical weathering, formation of secondary products such as clays, and element mobility, either by leaching or mineral sorting. Geographical distribution (based on ProMine Mineral Database, Cassard et al., 2012, 2015) of the mineralised areas are shown in Figs. 4a, 5a and 6a for Sb, W and Li, respectively, and the maps of Sb, W and Li in the hot aqua regia extraction of agricultural soil samples are correspondingly displayed in Figs. 4b, 5b and 6b, respectively.

3.2.1. Spatial distribution of Sb

The Ap map of Sb in the hot aqua regia extraction show one of the most striking differences in element concentration between the Ap soil of all analysed elements/parameters (Fig. 4a) between northern (median 0.11 mg/kg) and southern Europe (median 0.35 mg/kg). It is worth noting the difference in Sb concentrations between the upper continental crust and world soil, 0.75 and 0.9 mg/kg, respectively, compared to values in Ap soil. This pronounced disparity of Sb concentrations is most likely an effect of glaciation, soil age and weathering. Soil pH is generally lower in northern than in southern Europe facilitating thus the removal and accumulation of many elements including Sb from soil. Low pH and/or high content of organic matter are two main factors controlling the fate of Sb in soil. Interestingly, Ap soil samples collected in the far north over Archaean bedrock in Fennoscandia are characterised by the lowest Sb contents in Europe, a feature also known from various local studies and national geochemical surveys, e.g., Andersson et al. (2014). It seems, that soil developed on old cratonic areas, such as the Fennoscandian Shield and East European Platform with the oldest bedrock in Europe, are highly depleted in Sb in comparison with soil formed from parent materials composed of younger bedrock in western and southern Europe. Even though Sb mineralisation is usually located within granitic bodies, the pristine granitic massifs at several locations in Europe show very low Sb contents in overlying soil, e.g., in NE Sardinia, northern Portugal and western-central Spain (Fig. 4b). The enrichment in Sb occurs in soil developed on sedimentary rocks such as shale, mudstone and young argillaceous rocks. Soil within the Carpathian Belt, where flysch-type rocks dominate, has elevated Sb contents. More rarely, Sb can substitute Fe and occurs as trace element in minerals typical of mafic rocks (e.g., in olivine) and, therefore, certain Sb enrichment may occur in areas where mafic to intermediate volcanic rocks occur, e.g., in Italy, France (Massif Central) and Czech Republic (part of the Bohemian Massif) exist. A couple of Sb anomalies in Italy are associated with the Roman and Neapolitan alkaline volcanic provinces (Nos. 36 & 37, Fig. 4b).

In the hypergene zone, Sb is often associated with Fe and Al oxides/hydroxides, and can be sorbed onto silicate grains, representing a potentially bioavailable and extractable fraction (Gal et al., 2007). Such a process may be possibly the cause of Sb enrichment in soil in warm Mediterranean climates.

3.2.2. Spatial distribution of W

The geochemical map of W shows an interesting distribution pattern, which is different from that of Sb (Fig. 5b). Though the northern European Ap soil displays somewhat lower W values (median 0.058 mg/kg) than those from southern Europe (median 0.083 mg/kg), the boundary does not exactly follow the limit of the last glaciation. This is due to the many high values observed in German soil and, in general, in central Europe. In Germany, several anomalies (from Hannover to the border of The Netherlands) coincide with the occurrence of sedimentary iron ore deposits. Poland and Ukraine are in contrast marked by very low W concentrations in Ap soil. This can be explained by the presence of aeolian deposits, coversands and loess, deposited prior to, and just after, the last glaciation maximum and are of Weichselian age (Zeeberg, 1998). These deposits are rich in Hf and Zr (Scheib et al., 2012) but depleted in fine-grained fraction W, and the primary W minerals, such a scheelite and wolframite, are not easily dissolved by traditional hot acid extractions. In fact, most of the elevated W background in Europe is observed in areas underlain by crystalline bedrock.

Many granitic intrusions (see Fig. 5b; Cornwall in south-west England (No. 13), northern Portugal (Nos. 49 & 50), Massif Central (No. 39) in France, for example) are clearly marked by W anomalies, as are the Roman and Neapolitan alkaline volcanic rocks in Italy (No. 31). The Vosges (No. 38) and the Alpine region (especially the western part, Nos. 27, 28 & 29) are marked by enhanced W concentrations. This is most likely related to the crystalline massifs and to the extensive tectonic lines with associated magmatic rocks (Rhône-Simplon-Insubria-Periadriatic Line) and metamorphic rocks (trace W concentrations are common in mica-rich rocks). In Sweden and Finland, the predominance of granitic bedrock (Fennoscandian Shield) over large parts of these countries is well reflected in somewhat enhanced W concentrations. The higher nappes in the Scandinavian Caledonides (mainly calcareous sedimentary rocks) and the Archaean bedrock in the north are characterised by low W soil concentrations. In eastern Finland, W depletion delineates the location of so called greenstone belts. Generally, low W contents in soil occur in areas with glacial drift (central Europe) and with transported calcareous materials, e.g., in Denmark.

It is worth noting that the geochemical mobility of W is different

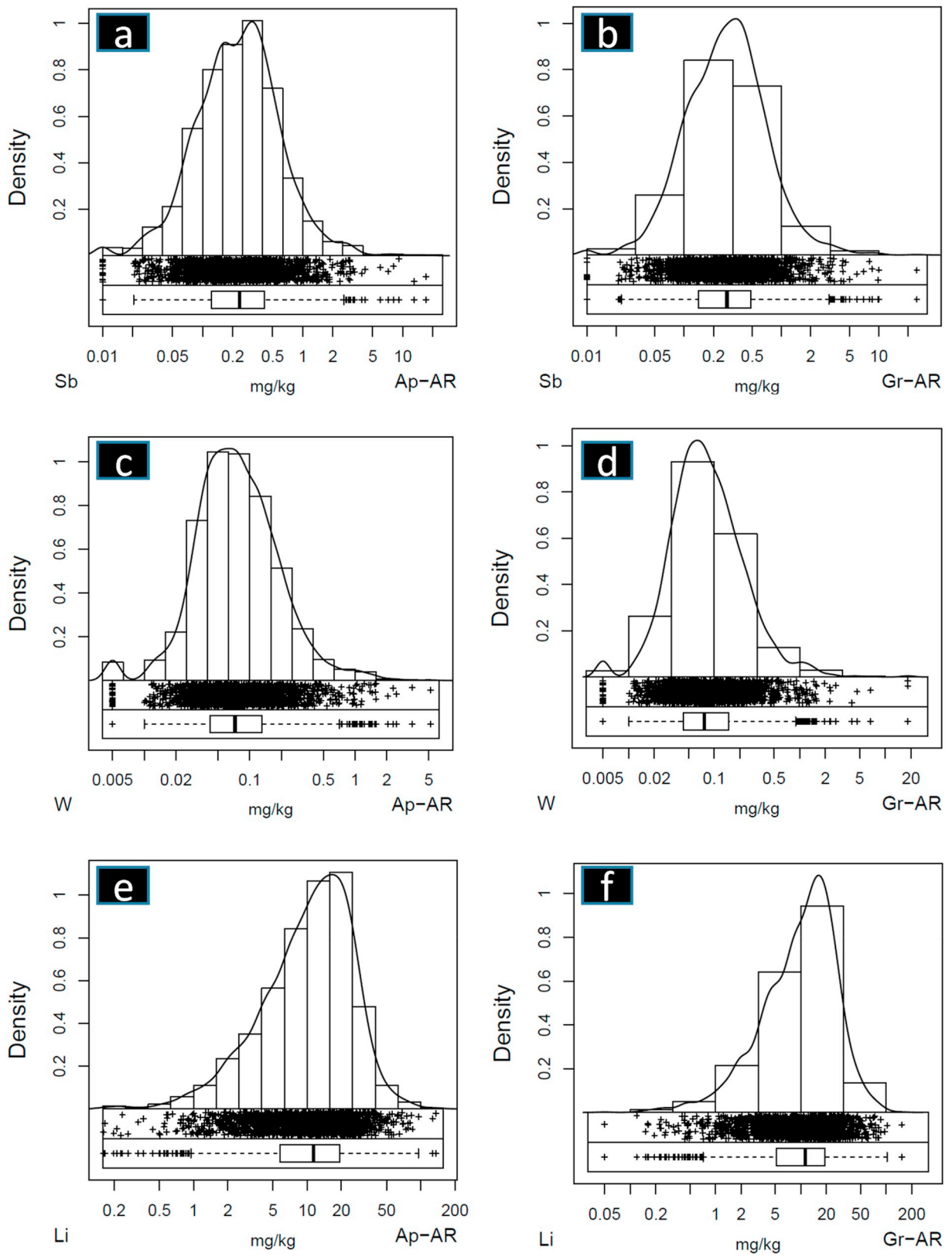

Fig. 3. Combined plot of histogram, density trace, one-dimensional scattergram and boxplot distribution in European Ap and Gr samples following a hot aqua regia extraction for the three elements Sb (a for Ap and b for Gr samples), W (c for Ap and d for Gr samples), Li (e for Ap and f for Gr samples).

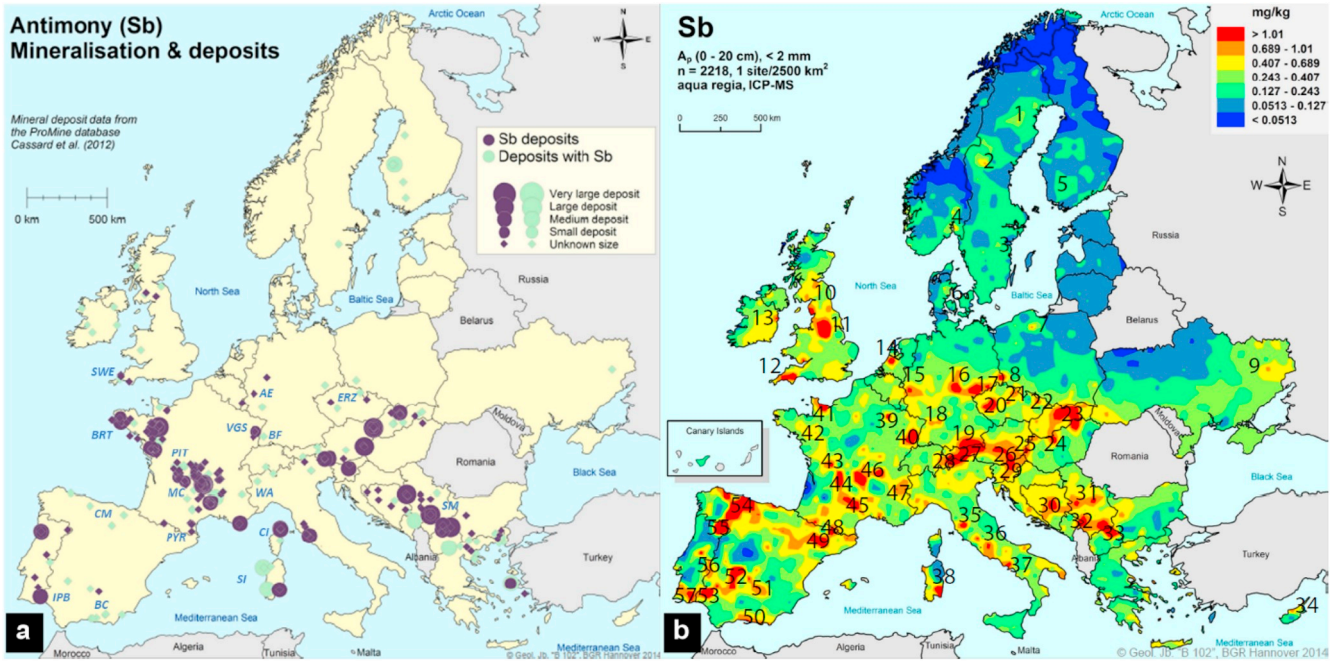

Fig. 4. (a) Distribution of Sb-bearing ore deposits in Europe (based on the ProMine Mineral Database; Cassard et al., 2012, 2015; Demetriades and Reimann, 2014). Abbreviations of mineralised districts: AE: Ardennes–Eifel; BC: Betic Cordillera; BF: Black Forest; BRT: Brittany; CI: Corsica; CM: Cantabrian Mts.; ERZ: Erzgebirge (Ore Mts.); IPB: Iberian Pyrite Belt; MC: Massif Central; PIT: Poitou; PYR: Pyrenees; SI: Sardinia; SM: Serbo-Macedonian ore district; SWE: South-west England ore district; VGS: Vosges; WA: Western Alps; (b) Soil geochemical map for hot aqua regia extractable Sb concentrations in ploughed agricultural soil (Ap, N = 2108). Numbered anomalies are listed in Table 3.

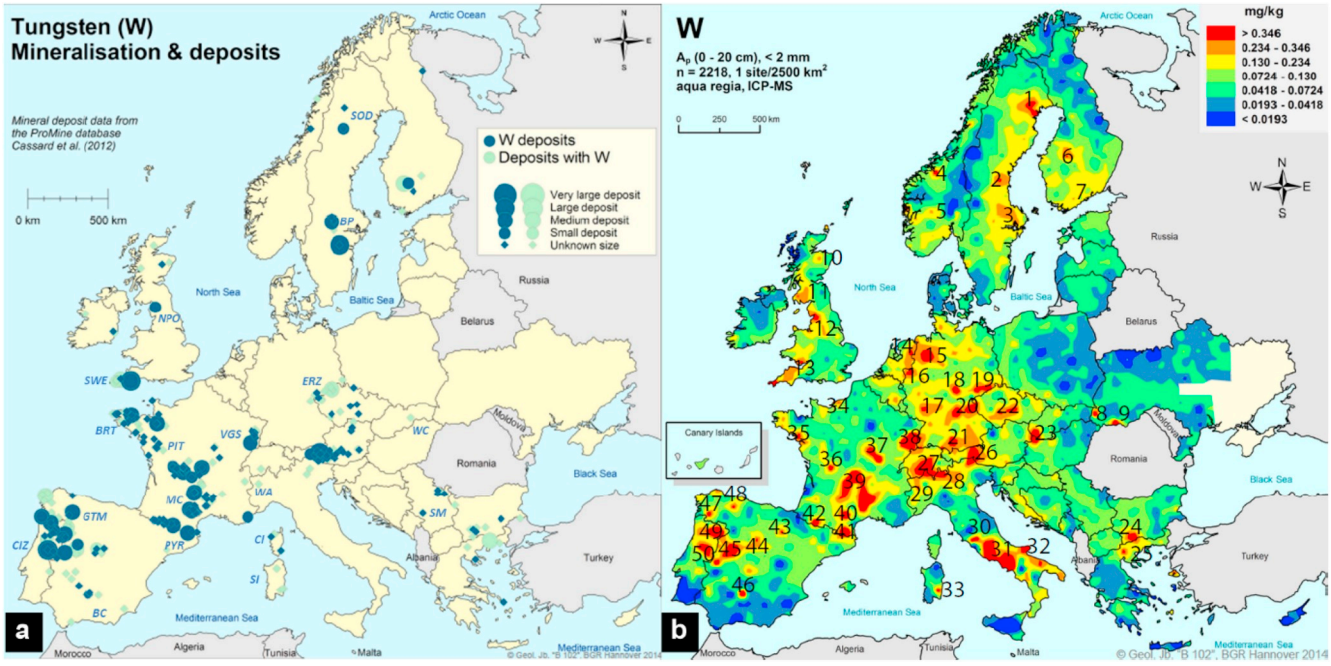

Fig. 5. (a) Distribution of W-bearing ore deposits in Europe (based on the ProMine Mineral Database; Cassard et al., 2012, 2015; Demetriades and Reimann, 2014). Abbreviations of mineral districts: BC: Betic Cordillera; BP: Bergslagen ore province; BRT: Brittany; CI: Corsica; CIZ: Central Iberian ore zone; ERZ: Erzgebirge (Ore Mts.); GTM: Galicia-Trás-os-Montes zone; MC: Massif Central; NPO: North Pennine orefield; PIT: Poitou; PYR: Pyrenees; SI: Sardinia; SM: Serbo-Macedonian ore district; SOD: Skellefte ore district; SWE: South-west England ore district; VGS: Vosges; WA: Western Alps; WC:Western Carpathians (b) Soil geochemical map for hot aqua regia extractable W concentrations in ploughed agricultural soil (Ap, N = 2108). Numbered anomalies are listed in Table 4.

from that of Sb; W is mobile under oxidising conditions in alkaline waters and tends to adsorb to Mn-oxides, clay minerals and binds to organic matter. Primary W exists almost exclusively in the form of tungstate minerals (scheelite $CaWO_4$, wolframite [Fe/Mn]WO_4), which are resistant to weathering. Under specific conditions, the formation of soluble W complexes, with many inorganic and organic ligands, enhance its mobility in the surface and subsurface aquatic environment (Koutsospyros et al., 2006).

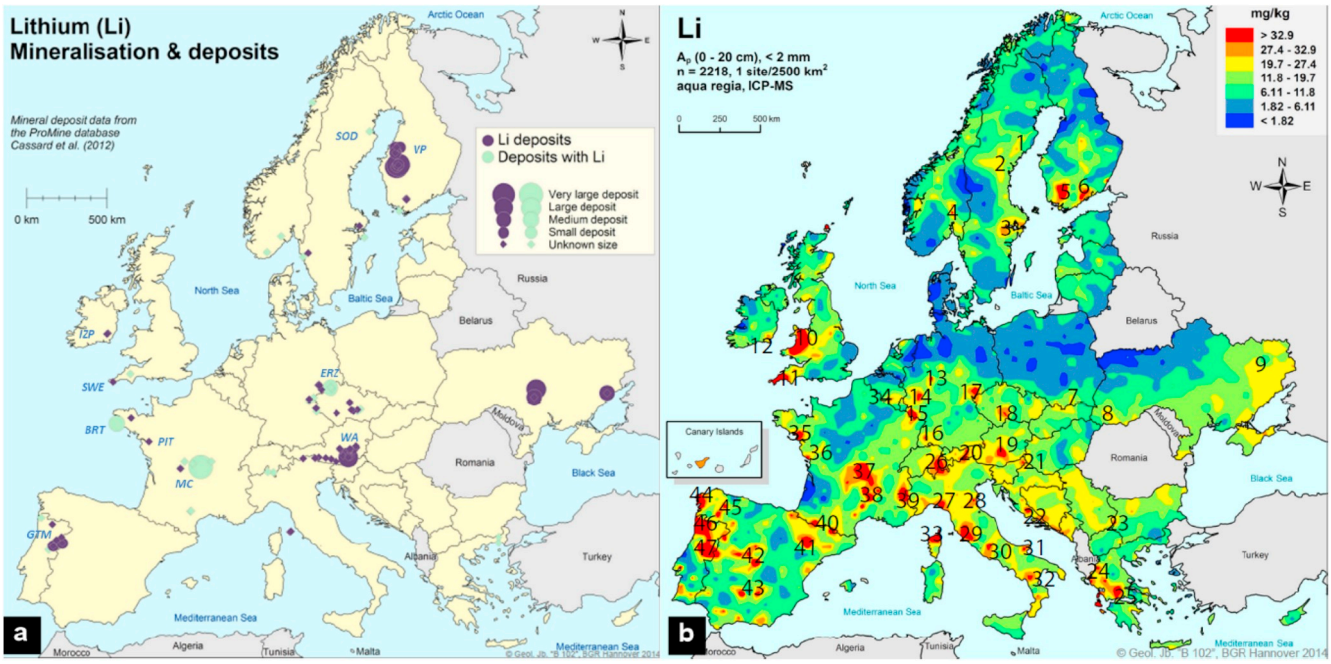

Fig. 6. (a) Distribution of Li-bearing ore deposits in Europe (based on the ProMine Mineral Database; Cassard et al., 2012, 2015; Demetriades and Reimann, 2014). Abbreviations of mineral districts: BRT: Brittany; ERZ: Erzgebirge (Ore Mts.); GTM: Galicia-Trás-os-Montes zone; IZP: Irish Zn–Pb ore district; MC: Massif Central; PIT: Poitou; SOD: Skellefte ore district; SWE: South-west England ore district; VP: Vihanti–Pyhäsalmi ore district; WA: Western Alps. (b) Soil geochemical maps for hot aqua regia extractable Li concentrations in ploughed agricultural soils (Ap, N = 2108). Numbered anomalies are listed in Table 5.

3.2.3. *Spatial distribution of Li*

The aqua regia extractable Li map displays typical GEMAS spatial distribution patterns (observed for many elements), with predominantly low concentrations in Ap soil in northern Europe (median 6.4 mg/kg Li) and evidently higher values in southern Europe (median 15 mg/kg Li; Fig. 6a). The maximum extent of the last glaciation is visible as a discrete concentration break on the Ap geochemical map of Li (Fig. 6b). The principal Li anomalies are spatially associated with granitic rocks throughout Europe, e.g., northern Portugal (Nos. 46, 47), Massif Central (Nos. 37 & 38) in France, Wales (No. 10), south-west England (No. 11). While in Fennoscandia the Central Scandinavian Clay Belt (Ladenberger et al., 2014) is clearly visible (Nos. 3 & 5), and this feature emphasises the tendency of Li to bind to clay (although developed on the crystalline, mainly granitic bedrock). The Alpine Region (especially the western part) is marked by enhanced Li concentrations (Nos. 26 & 30). This is most likely related to the crystalline massifs and to the extensive tectonic lines with associated magmatic rocks (Rhône-Simplon-Insubria-Periadriatic Line). In northern Portugal, the extensive Li anomaly (Nos. 46 & 47, Fig. 6b) is related to the occurrence of Li-pegmatites. The anomaly in the Wolfsberg area in Austria (No. 26) is also associated with Li-pegmatites with no known relation to any granite. High Li values occurring over karst limestone areas in southern Europe (Croatia, No. 22) are possibly due to secondary Li enrichment attributed to climatic conditions, and to phosphorite and bauxite occurrences (Hellas, Nos. 24 & 25). In arid areas, Li can be enriched via precipitation (together with other evaporite minerals). Lithium's tendency to bind to clay leads to enrichment in fine-grained sedimentary rocks, both young and unaltered and those metamorphosed into schist. Additionally, Li occurs in trace amounts in mica and amphibole minerals, and soil with mica-rich parent materials (such as mica schist) can have high Li concentrations.

The Li concentration is compared with the clay content in Fig. 7. The classical representation of Li concentration (mg/kg) *vs.* clay content (%) evidenced the existence of heteroscedasticity in the data. To overcome this, the Li concentrations are plotted with logarithmic scaling and the clay contents are expressed as a binary logit function, i.e., a logistic transformation according to log[P/(100-P)] where P is the clay content. A clear trend is observed in Fig. 7, less visible, however, for soil developed on coarse-grained sandy deposits ('quartz') and calcareous rock ('chalk'), since these parental materials do not produce clay minerals under weathering processes. Better correlation occurs in soil developed on greenstone ('green') and Precambrian bedrock (granitic gneiss - 'prec') – these parent materials are sources to thick clay overburden as a result of weathering, especially in warm and humid climate.

The correlation between Li and Fe and Al was earlier reported by Reimann et al. (2012a). The strong Li–Al correlation can be explained by the fact that kaolinite, the most aluminous mineral, easily fixes large amounts of Li compared to other minerals such as illite or chlorite (Tardy et al., 1972). Using a selection of regional data from the GEMAS project (e.g., from Nordic countries), this very strong relationship between Li and Al is shown (Fig. 8).

3.3. *Emerging critical elements in soil as mineral potential indicators*

Nowadays, high-tech elements are rarely mined as a main ore. Most often, they are co-products from the principle ore (e.g., Zn, Fe, Cu). In order to identify economic resources of high-tech materials, Sb, W and Li from agricultural soil (Ap) are used as proxies, and it is here discussed whether the geochemical anomalies in soil can be utilised for mineral exploration purposes. It is vitally important to be able to discriminate 'real' anomalies, high element concentrations related to potential economic mineralisation, from secondary enrichment caused by weathering, climate, contamination, etc. Historical and inactive mining regions can be of interest since there are a strong political and environmental reasons to utilise mining wastes, such as tailings and waste heaps.

The majority of Sb, W and Li GEMAS geochemical anomalies in Ap soil can be directly related to known mineralisation and ore deposits (Figs. 4 to 6 and Tables 3 to 5). Except for deposits in the Fennoscandian Shield, most of the ore deposits in Europe are located within Palaeozoic to Caenozoic tectonic units and are related to respective orogenic events, e.g., in the Ordovician (Caledonian orogeny), Carboniferous (Variscan orogeny) and Tertiary (Alpine Orogeny). Active volcanism, regional

metamorphism and hydrothermal activity often accompanied these events. In western, central and southern Europe, most mineralisation is located in Variscan and Alpine units, while within the Fennoscandian Shield in northern Europe the majority occurs in Proterozoic (Sweden, Finland) and Caledonian (Sweden and Norway) terranes.

In order to evaluate the mineral potential of Sb, W and Li, GEMAS maps have been compared to the ProMine Mineral Database and European Minerals Knowledge Data Platform (Cassard et al., 2012, 2015, which is based on the ProMine Mineral Database; http://minerals4eu.brgm-rec.fr/) (Tables 3 to 5). These online databases contain compiled information about mineralisation and ore deposits for Europe and are often used by companies and policy makers. While most mineralisation is not reflected in the Ap soil geochemistry, there are several relatively large anomalies which cannot be easily explained by the ProMine Mineral Database. Such an example is Sb anomaly No. 39 in eastern France, which coincides with a Pb anomaly (No. 22 in Reimann et al., 2012b) where there is no known mineralisation, no smelter, no major city but correlate well with the proximity to Verdun, a small city made famous because of a fierce First World War (WW1) battle. Anomalies of Sb (No. 49) and Li (No. 41) are also unexplained by the ProMine Mineral Database and they appear to be significant in northern Spain. These geochemical anomalies can be found in the Geochemical Atlas of Spain (Locutura et al., 2012) and they seem to correlate with known polymetallic mineralisation (Pb–Zn–Cu–Ag–Sb–Bi–As–W–Au) in the pre-Pyrenean and Pyrenean region and to the existence of clays and evaporitic salts north of Zaragoza city and 100 km east in the Cardona-Suria Salt mines.

Interestingly, many anomalies of Sb, W and Li can be correlated to the ProMine Mineral Database deposits, which do not list these particular elements as associated commodities, e.g., Nordli Mo deposit in Norway and base-metal sulphide deposits in northern Sweden (Skellefte district). Additionally, a difference in background concentrations between northern and southern Europe requires a separate interpretation of Fennoscandian countries by taking into account the local background levels.

3.3.1. *Antimony in soil as a mineral potential indicator*

By studying the Sb maps in more detail (Fig. 4a and b), it can be observed that most of the identified anomalies correspond with known mineral belts or ore deposits (Table 3). The highest Sb contents in Ap soil occur in Portugal where several known Sb occurrences are located, for example, within the so called Iberian Pyrite Belt, in south-eastern Portugal. In Austria, an Sb anomalous region stretches in a form of a belt in the Alps and coincides with many known mineralised occurrences and historical mines. The Massif Central in France with its extensive hydrothermal mineralisation stands out as an anomaly, as does the Iberian Pyrite Belt (southern Spain and Portugal), the Vosges (French and German border), Ardennes-Eifel (Germany), the Ore Mountains (German and Czech border), Bohemian Forest (Czech Republic), Carpathians (Slovakia), and the Pennine and south-west England ore-fields in the United Kingdom. High Sb contents in Ap soil occur also in the Balkan countries, Bosnia and Herzegovina, Serbia (with Kosovo), North Macedonia and Hellas, and they all are related to various types of mineralisation, mainly polymetallic with Pb–Zn–Cu, the Serbo-Macedonian mineralised zone.

Due to strong contrast in Sb concentrations between northern and southern Europe, the Sb concentrations in the soil of Fennoscandia, Estonia, Latvia, Lithuania, northern Poland, Denmark and northern Germany should be displayed as a separate data set (Fig. 9). In Fennoscandia, relatively high Sb concentrations are mainly related to polymetallic mineralisation, e.g., Pb–Zn–As deposits in northern Sweden (Skellefte district), Sb, Bi, Au and As mineralisation north-west of Luleå,

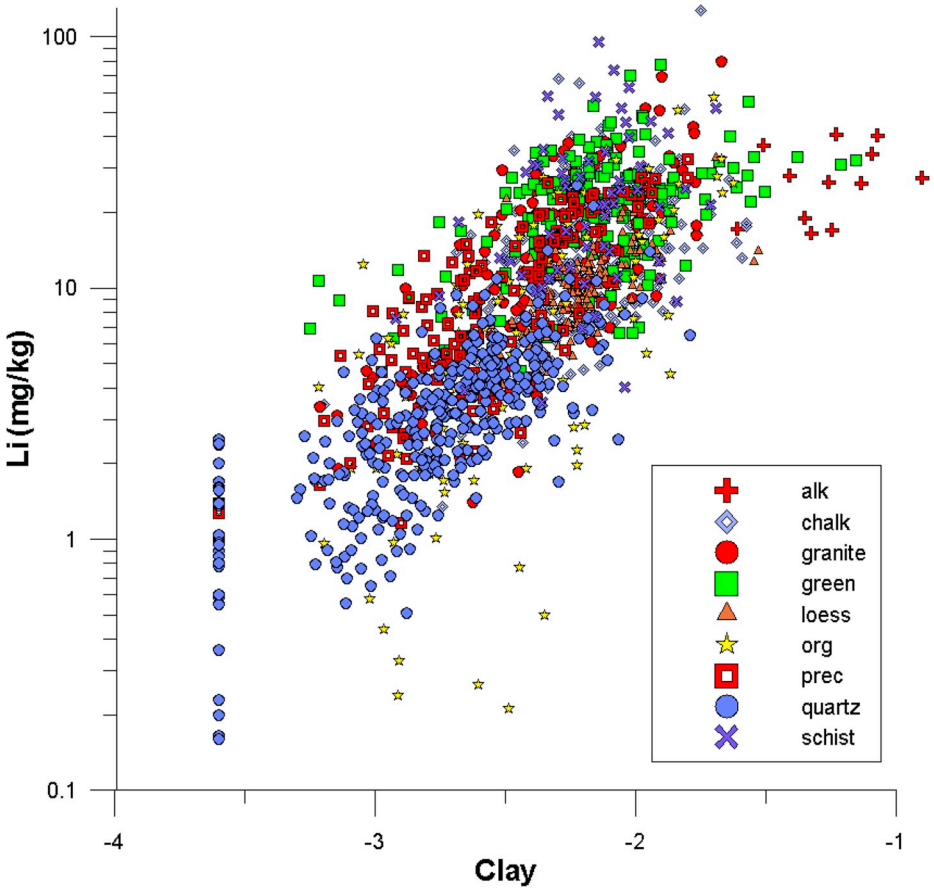

Fig. 7. Plot of clay (%) and Li (mg/kg) contents in European Ap soil samples. Data are classified according to the ten geological parent material subgroups (Reimann, 2012a, b), comprising alk: alkaline rock; chalk: calcareous rock; granite: granitic bedrock; green: greenstone, basalt, mafic bedrocks; loess: loess; org: organic soil; other: unclassified bedrock; prec: predominantly Precambrian granitic-gneiss; quartz: soil developed on coarse-grained sandy deposits; schist: schist.; the category 'other' in the original classification has not been plotted on the graph. (For interpretation of the references to colour in this figure legend, the reader is referred to the Web version of this article.)

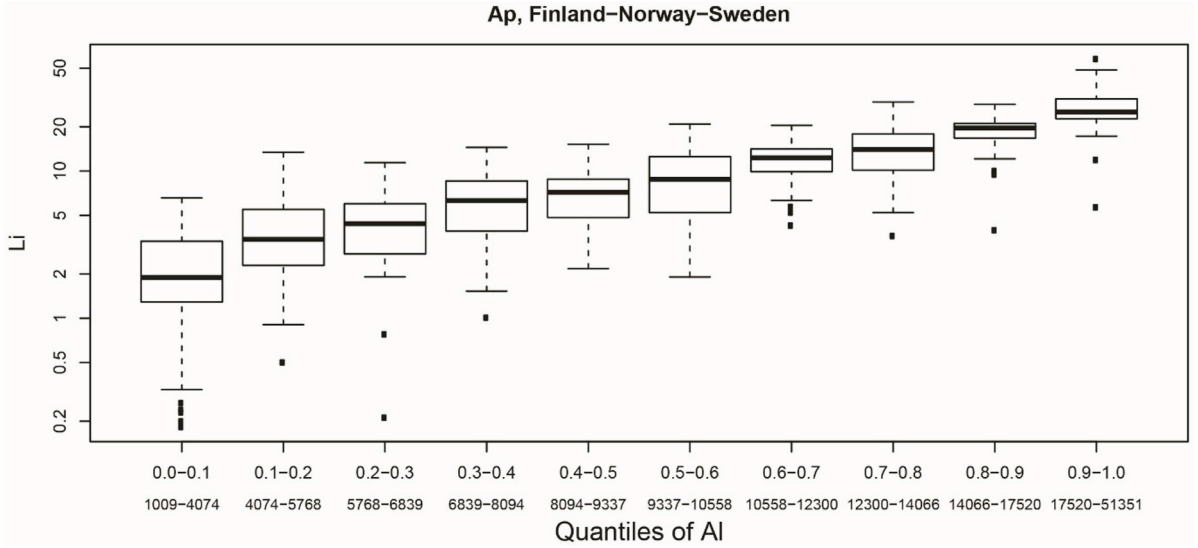

Fig. 8. Multiple boxplots showing relationship between Li concentrations (mg/kg) and Al quantiles in Ap GEMAS samples from Sweden, Finland and Norway (Ladenberger et al., 2013).

and in central Sweden (Bergslagen district). Known Zn–Pb mineralised occurrences in SW Scania in southern Sweden are indicated by a large Sb geochemical anomaly in grazing land soil. High Sb concentrations in two Ap soil samples are unexplained; one in the northernmost Sweden within the Archaean bedrock and the other in SE Sweden (Småland, near Oskarshamn). The remarkable enrichment in Sb in the fine-grained sedimentary rocks (mainly in black shale, e.g., in the Lower Allochthon of the Caledonides), although appearing very promising, has potentially no economic significance mainly because Sb is dispersed at low levels and does not form economic ore-bodies, as its mining is difficult and requires processing of large volumes of rocks. In Norway, large Sb anomalies are closely related to mineralisation within the Oslo Rift and in SW Norway with some sulphide polymetallic deposits (Fig. 9).

Economic occurrences of Sb in Europe are mainly associated with sulphide deposits, and Sb can be used as a pathfinder element for sulphide mineral deposits (Boyle, 1974; Boyle and Jonasson, 1984). Another example is from deposits in Austria that were economic in their time related to their mono-mineral characteristic (stibnite). Antimony is also used together with As and Bi as a pathfinder element for Au mineralisation (Boyle, 1974; Boyle and Jonasson, 1984; Plant et al., 1989). In other words, using Sb, sulphide ores can be classified according to their potential for hosting by-products of economic importance.

Because many of the Sb-hosting deposits have been mined historically (e.g., in France), it is difficult to evaluate to what extent Sb anomalies are natural anomalies (due to the occurrence of the deposits themselves) or whether the extent of mining and smelting activities has accentuated originally very local anomalies. To answer the question 'natural or anthropogenic' in these areas, detailed studies would be needed in every single case. On the other hand, the size of an anomaly can be used as pathfinder for potential future recovery at the source (e.g., from past tailings). Otherwise, typical anthropogenic Sb anomalies related to urbanisation, although rare, they have been recognised near Amsterdam, Budapest, Rome and Naples. Additionally, interesting historical Sb impacts can be observed, e.g., in Naples region (Italy). The rather large Sb anomaly, apart from possibly being anthropogenic (Naples), coincides with the location of Europe's largest volcano – Vesuvius. Antimony occurs naturally in groundwater close to volcanoes, and Pompeii's proximity to Mount Vesuvius could have provided Sb concentrations in the water that were even higher than in a typical Roman city at the time. Antimony poisoning is known in this area from historical times. The Pb pipes in Pompeii, studied by archaeologists, contain Sb which was likely a cause of health problems among the residents (Charlier et al., 2017).

3.3.2. *Tungsten in soil as a mineral potential indicator*

Tungsten anomalies in European Ap soil are most pronounced in regions with granitic bedrock and associated with various types of mineralisation, especially Au (and Ag) and base metals hosted by granitic rocks (Fig. 5a and b). This is typical geological environment where various W ore deposits can be found, e.g., granitic intrusions in northern Portugal, Massif Central in France, Bohemian Massif in Czech Republic, the Vosges Mountains in eastern France and the Alpine region (mainly in Switzerland and western Austria). Scheelite and wolframite (often accompanied by cassiterite and fluorspar) are the economic sources of W, and they are mainly found in quartz-rich veins, pegmatites and skarn deposits. Most W deposits are of metasomatic or hydrothermal origin. Tungsten is used as a pathfinder for gold deposits. High W concentrations occur in Ap soil that overlies igneous and metamorphic rocks of the Fennoscandian Shield, mainly of Palaeoproterozoic age. In Scandinavia, the largest W anomalies occur in the Skellefte ore district, Bergslagen and sporadically along the coast of the Gulf of Bothnia. These anomalies reflect known W mineralisation occurring in granite, gneiss and quartz veins (together with U, Au, Ag and Li). In Lapland, anomalies occur within the so called Gold Line and they follow Sn, Mo, Cu, Fe, U and precious metal ore deposits with Au and Ag. The Bergslagen mining district comprises the most important W (scheelite) ore deposits in Sweden, which are located mainly in skarn-limestone, commonly in contact with Svecokarelian granitic rocks (Andersson et al., 2014).

By comparison with the ProMine mineral deposit map (Table 4; Fig. 5a and b), it can be observed that several strong anomalies are not reflected on the mineral deposits map, e.g., anomalies in NW Germany/Eastern Netherlands, SW Slovakia, central Italy, southern and central Germany, northern Sweden and central Finland. For example, an unexpectedly extensive W anomaly in central Italy (No. 31, Fig. 5b) might be related to the young volcanism. Other anomalies, such as No. 18 in the Thuringian Forest indicates that mining and exploration activities in this polymetallic province did not focus on W, which shows elevated soil concentrations. All these observations indicate that there is a high potential for discovering new W resources.

3.3.3. *Lithium in soil as a mineral potential indicator*

Lithium in agricultural soil (Table 5, Fig. 6a and b) shows its high concentrations predominantly in regions with granitic parent materials.

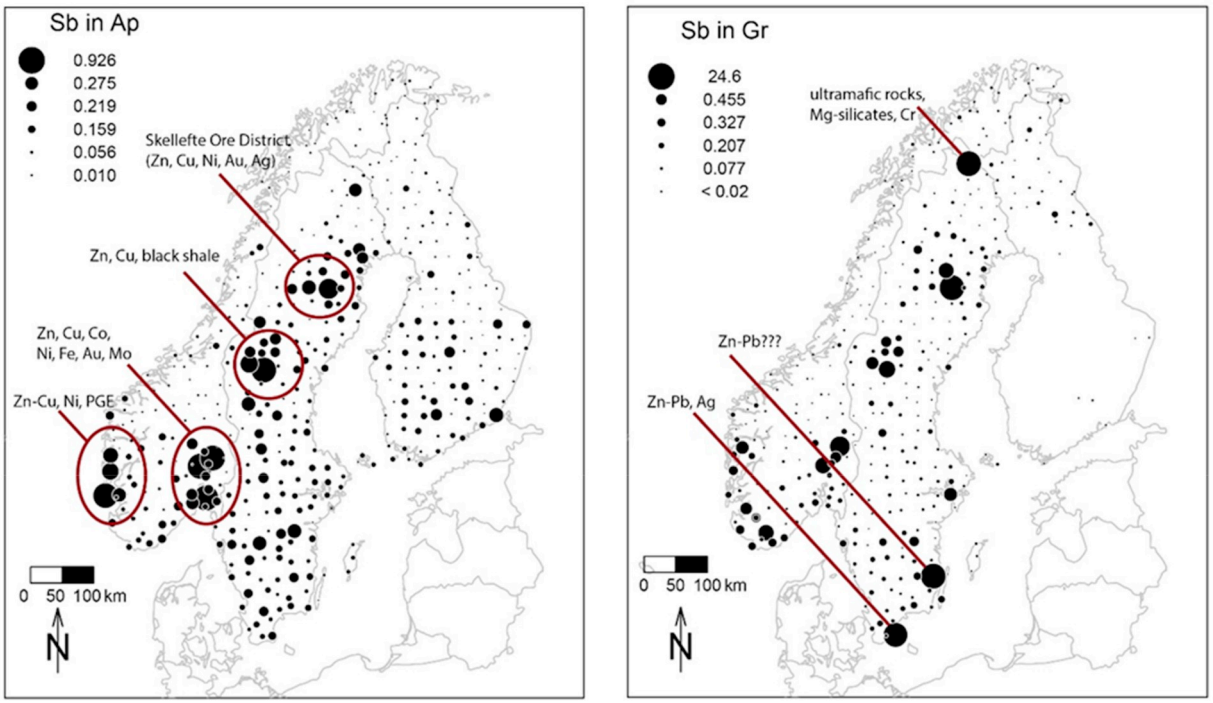

Fig. 9. Sb geochemical maps (mg/kg) in Ap (n = 453) and Gr (n = 350) soil of Norway, Sweden and Finland. Regional Fennoscandian percentile calculation allows clear detection of anomalies. Most of them can be explained by mineralisation or lithology.

A comparison between Li-bearing ore deposits in Europe and the Ap soil geochemical map for Li reveals that many anomalies are associated with Li-bearing mineralisation, especially with occurrences of LCT (Lithium-Cesium-Tantalum) pegmatites, for example, in the Galicia-Trás-os-Montes zone (anomalies No. 46 and 47 and in western Alps (anomaly No. 39). In NW Spain and northern Portugal, Li anomalies are closely associated not only with known Li mineralisation but also with Sn, W, Nb and Ta occurrences. These Li deposits in the Central Iberian Zone have been mined intensively in recent years and Portugal became the world's sixth largest Li producer (Roda-Robles et al., 2016). In northern Europe, high Li concentrations in Ap soil occur in regions with granitic parent materials (e.g., southern Finland), but also in till overburden enriched in postglacial and marine clay, for example, in central Sweden (see also Fig. 8). In southern Lapland, anomalies coincide with Au, W, Mo and scheelite mineralisation of the 'Gold Line' ore province. Recently, the Bergby deposit was discovered in central Sweden, which lies 25 km north of the town of Gävle with Li_2O averaging 1.71% and ranging from 0.01% to 4.65% (http://leadingedgematerials.com/leading-edge-materials-discovers-lithium-mineralization-in-outcrop-at-bergby-project-sweden/).

There is a clear correlation of Li with mica- and clay-rich soil (as reflected by Ga, Al, Cs, Rb) but also with some Fe-rich phases, which can be a result of both weathering and presence of more mafic parent materials (correlation together with Fe, Cr, Co, Sc). High correlation with chalcophile elements such as Zn, In, Tl, Cu makes geochemical behaviour of Li in soil more complicated and requires careful interpretation at the regional to local scale. Lithium anomalies are more difficult to follow in the ProMine Mineral Database (Cassard et al., 2012, 2015). There are several relatively extensive anomalies, which do not have a direct explanation with respect to the ProMine Mineral Database, e.g., Li anomaly in Wales (No. 10, Fig. 6) in the United Kingdom, Li anomalies in western Germany (Nos. 13 and 14), in W Hellas (Nos. 24 and 25) and in NE Spain (No. 41). Locally, high Li concentrations in Ap soil occur at Lisbon city limits in the delta of the Tajo river, and in the vicinity of the brackish lagoons with brines near Ravenna in Italy, and they may have secondary and even anthropogenic origin. These enhanced secondary Li concentrations can be misleading when looking for economic Li occurrences.

3.3.4. *Combined Sb, W and Li anomalies in soil as mineral potential indicators*

Table 6 summarises the co-existing anomalies for Sb, W and Li. The most straightforward observation is that in several regions (Cornwall, Massif Central, Erzgebirge, and the Alps) all three commodities can be found close to one another and, thus, polymetallic ore provinces can be defined, even if the host rock is not of the same lithology and the ore-forming processes also differ.

4. Conclusions

The demand for 'high-tech' element resources stimulated efforts to find new deposits and even possibilities to extract them from active and historical mines throughout the world. The GEMAS data set offers European scale results for several so-called high-tech elements, and almost all listed on the Critical Raw Materials list by the European Commission (2017). Here, three of the high-tech elements, Sb, W and Li were used as

Table 6
Summary of co-existing Sb, W and Li anomalies.

Region	Sb	W	Li
Cornwall (United Kingdom)	12	13	11
Massif Central (France)	44–46	39	37–38
W Pyrennes (N Spain/S France)	48	42	40
Erzgebirge (E Germany/N Czech Republic	19	17	17
W Salzburg/Tyrol (Austria)	27	26	20
Brittany (NW France)		35	35
Central Portugal		50	47
Southern Czech Republic		18	22
SE France	47		39
NE Spain	49		41
E Ukraine	9		9
W France	43	36	
E France	40	38	

test elements. The geochemical distribution of Sb, W and Li in agricultural soil of Europe appears to be a useful starting tool for identifying areas for discovering new sources of high-tech elements. Most of the patterns observed on the geochemical maps of Sb, W and Li can be directly interpreted in terms of known ore deposits and mineralised occurrences and most of the anomalies reflect natural sources of these elements. Additionally, their spatial distribution seems to be modified by weathering type and intensity, Quaternary history and climate, like, for example, the clear difference in element concentrations between northern and southern Europe. The chemical composition of agricultural soil represents largely the primary mineralogy of the source parent material, with superimposed effects of pre- and post-depositional chemical weathering, formation of secondary products such as clays, and element mobility. For Sb, the most promising are regions with known sulphide mineralisation, while for Li and W, regions with crystalline bedrock and evolved granitic rocks should be of interest.

Natural background concentrations of Sb, W and Li in agricultural soil define areas of interest and their relationship to mineralisation, rock types and mining centres, and provide important ground for further investigations. The application of GEMAS soil data to mineral exploration is promising, especially as most of the Sb, W and Li anomalies can be explained by known and mapped mineralisation (such as the ProMine Mineral Database and national registers). In conclusion, several unexplained anomalies require more detailed geochemical surveys, these could shed light on potential mineral resources that have to date remained undiscovered.

Declaration of competing interest

The authors declare that they have no known competing financial interests or personal relationships that could have appeared to influence the work reported in this paper.

Acknowledgments

The GEMAS project is a cooperative project of the EuroGeoSurveys Geochemistry Expert Group with a number of outside organisations (e.g., Alterra, The Netherlands; Norwegian Forest and Landscape Institute; Research Group Swiss Soil Monitoring Network, Swiss Research Station Agroscope Reckenholz-Tänikon, several Ministries of the Environment and University Departments of Geosciences, Chemistry and Mathematics in a number of European countries and New Zealand; ARCHE Consulting in Belgium; CSIRO Land and Water in Adelaide, Australia). The analytical work was co-financed by the following industry organisations: Eurometaux, European Borates Association, European Copper Institute, European Precious Metals Federation, International Antimony Association, International Lead Association-Europe, International Manganese Institute, International Molybdenum Association, International Tin Research Institute, International Zinc Association, The Cobalt Development Institute, The Nickel Institute, The (REACH) Selenium and Tellurium Consortium and The (REACH) Vanadium Consortium. The Directors of the European Geological Surveys, and the additional participating organisations, are thanked for making sampling of almost all of Europe in a tight time schedule possible. The Federal Institute for Geosciences and Natural Resourced (BGR), the Geological Survey of Norway and SGS (Canada) are thanked for special analytical input to the project.

Appendix A. Supplementary data

Supplementary data to this article can be found online at https://doi.org/10.1016/j.apgeochem.2019.104425.

References

Albanese, S., Sadeghi, S., Lima, A., Cicchella, D., Dinelli, E., Valera, P., Falconi, M., Demetriades, A., De Vivo, B., the GEMAS Project Team, 2015. GEMAS: chromium, Ni, Co and Cu in agricultural and grazing land soil of Europe. J. Geochem. Explor. 154, 81–93.

Aitchison, J., 1986. The Statistical Analysis of Compositional Data. Chapman & Hall, London, p. 416.

Ali, S.H., Giurco, D., Arndt, N., Nickless, E., Brown, E., Demetriades, A., Durrheim, R., Enriquez, M.A., Kinnaird, J., Littleboy, A., Meinert, L.D., Oberhänsli, R., Salem, J., Schodde, R., Schneider, G., Vidal, O., Yakovleva, N., 2017. Mineral supply for sustainable development requires resource governance. Nature 543, 367–372.

Andersson, M., Carlsson, M., Ladenberger, A., Morris, G., Sadeghi, M., Uhlbäck, J., 2014. Geokemisk Atlas Över Sverige (Geochemical Atlas of Sweden). Geological Survey of Sweden, p. 210. http://doi.org/10.13140/2.1.1341.6642.

Bednar, A.J., Jones, W.T., Chappell, M.A., Johnson, D.R., Ringelberg, D.B., 2010. A modified acid digestion procedure for extraction of tungsten from soil. Talanta 80, 1257–1263.

Belzile, N., Chen, Y.-W., Wang, Z., 2001. Oxidation of antimony (III) by amorphous iron and manganese oxyhydroxides. Chem. Geol. 174, 379–387.

Bertrand, G., Cassard, D., Arvanitidis, N., Stanley, G., EuroGeoSurveys Mineral Resources Expert Group, 2016. Map of critical raw material deposits in Europe. Energy Procedia 97, 44–50. https://doi.org/10.1016/j.egypro.2016.10.016.

Birke, M., Reimann, C., Rauch, U., De Vivo, B., Halamić, J., Klos, V., Gosar, M., Ladenberger, A., 2014. Distribution of cadmium in european agricultural and grazing land soil (Chapter 5). In: Reimann, C., Birke, M., Demetriades, A., Filzmoser, P., O'Connor, P. (Eds.), Chemistry of Europe's Agricultural Soils – Part B: General Background Information and Further Analysis of the GEMAS Data Set. Geologisches Jahrbuch (Reihe B103). Schweizerbarth, Hannover, pp. 89–115.

Birke, M., Reimann, C., Fabian, K., 2014. Analytical methods used in the GEMAS project (Chapter 5). In: Reimann, C., Birke, M., Demetriades, A., Filzmoser, P., O'Connor, P. (Eds.), Chemistry of Europe's Agricultural Soils – Part A: Methodology and Interpretation of the GEMAS Data Set. Geologisches Jahrbuch (Reihe B102). Schweizerbarth, Hannover, pp. 41–46.

Birke, M., Rauch, U., Stummeyer, J., 2015. How robust are geochemical patterns? A comparison of low and high sample density geochemical mapping in Germany. J. Geochem. Explor. 154, 105–128.

Birke, M., Reimann, R., Oorts, K., Rauch, U., Demetriades, A., Dinelli, E., Ladenberger, A., Halamić, J., Gosar, M., Jähne-Klingberg, F., The GEMAS Project Team, 2016. Use of GEMAS data for risk assessment of cadmium in European agricultural and grazing land soil under the REACH Regulation. Appl. Geochem. 74, 109–121.

Birke, M., Reimann, C., Rauch, U., Ladenberger, A., Demetriades, A., Jähne-Klingberg, F., Oorts, K., Gosar, M., Dinelli, E., Halamic, J., The GEMAS Project Team, 2017. GEMAS: cadmium distribution and its sources in agricultural and grazing land soil of Europe - original data versus clr-transformed data. J. Geochem. Explor. 173, 13–30.

Bölviken, B., Kullerud, G., Loucks, R.R., 1990. Geochemical and metallogenic provinces: a discussion initiated by results from geochemical mapping across northern Fennoscandia. J. Geochem. Explor. 39, 49–90. https://doi.org/10.1016/0375-6742(90)90069-M.

Bowen, H.J.M., 1979. Environmental Chemistry of the Elements. Academic Press, London, New York, p. 333.

Boyle, R.W., 1974. Elemental associations in mineral deposits and indicator elements of interest in geochemical prospecting. Energy, Mines and Resources Canada. Geol. Surv. Pap. 74–45, 40. https://doi.org/10.4095/102553.

Boyle, R.W., Jonasson, I.R., 1984. The geochemistry of antimony and its use as an indicator element in geochemical prospecting. J. Geochem. Explor. 20, 223–302.

Bringezu, S., Potocnik, J., Schandl, H., Lu, Y., Ramaswami, A., Swillin, M., Suh, S., 2016. Multi-scale governance of sustainable natural resource use—challenges and opportunities for monitoring and institutional development at the national and global level. Sustainability 8 (778), 1–25, 2016.

Buccianti, A., Pawlowsky-Glahn, V., Mateu-Figueras, G. (Eds.), 2006. Compositional Data Analysis in the Geosciences: from Theory to Practice. Geological Society, London, p. 224.

Buchert, M., Schüler, D., Bleher, D., 2009. Critical Metals for Future Sustainable Technologies and Their Recycling Potential. DTI/1202/PA. UNEP DTIE, Sustainable Consumption and Production Branch, Paris. http://www.unep.fr/shared/publications/pdf/DTIx1202xPA-Critical%20Metals%20and%20their%20Recycling%20Potential.pdf.

Buschmann, J., Sigg, L., 2004. Antimony(III) binding to humic Substances: influence of pH and type of humic acid. Environ. Sci. Technol. 38, 4535–4541.

Caritat, P. de, Cooper, M., 2011. National Geochemical Survey of Australia: Data Quality Assessment, Geoscience Australia, vol. 1. Australian Government, Canberra, pp. 1–268. Record 2011/21, GeoCat # 71971.

Caritat, P. de, Cooper, M., 2011. National Geochemical Survey of Australia: Data Quality Assessment, Geoscience Australia, vol. 2. Australian Government, Canberra, pp. 269–478. Record 2011/21, GeoCat # 71971.

Caritat, P.de, Cooper, M., 2011. National Geochemical Survey of Australia: the Geochemical Atlas of Australia, Geoscience Australia, vol. 1. Australian Government, Canberra, pp. 1–268. Record 2011/20, GeoCat # 71973.

Caritat, P.de, Cooper, M., 2011. National Geochemical Survey of Australia: the Geochemical Atlas of Australia, Geoscience Australia, vol. 2. Australian Government, Canberra, pp. 269–557. Record 2011/20, GeoCat # 71973.

Cassard, D., Bertrand, G., Maldan, F., Gaàl, G., Kaija, J., Aatos, S., Angel, J.M., Arvanitidis, N., Ballas, D., Billa, M., Christidis, C., Dimitrova, D., Eilu, P., Filipe, A., Gazea, E., Inverno, C., Kauniskangas, E., Maki, T., Matos, J., Meliani, M., Michael, C.,

Mladenova, V., Navas, J., Niedbal, M., Perantonis, G., Pyra, J., Santana, H., Serafimovski, T., Serrano, J.J., Strengell, J., Tasev, G., Tornos, F., Tudor, G., 2012. ProMine pan-European mineral deposit database: a new dataset for assessing primary mineral resources in Europe. In: Workshop on: Mineral Resources Potential Maps: A Tool for Discovering Future Deposits. 12th–14th March 2012, Nancy, France, Proceedings, pp. 9–13.

Cassard, D., Bertrand, G., Billa, M., Serrano, J.J., Tourlière, B., Angel, J.M., Gaál, G., 2015. ProMine mineral databases: new tools to assess primary and secondary mineral resources in Europe (Chapter 2). In: Weihed, P. (Ed.), 3D, 4D and Predictive Modelling of Major Mineral Belts in Europe. Mineral Resource Reviews. Springer International Publishing, pp. 9–58. https://doi.org/10.1007/978-3-319-17428-0_2.

Charlier, P., Bou Abdallah, F., Bruneau, R., Jacqueline, S., Augias, A., Bianucci, R., Perciaccante, A., Lippi, D., Appenzeller, O., Rasmussen, K.L., 2017. Did the Romans die of antimony poisoning? The case of a Pompeii water pipe (79 CE). Toxicol. Lett. 281, 184–186.

Cicchella, D., Lima, A., Birke, M., Demetriades, A., Wang, X., De Vivo, B., 2013. Mapping geochemical patterns at regional to continental scales using composite samples to reduce the analytical costs. J. Geochem. Explor. 124, 79–91.

Cicchella, D., Albanese, S., Birke, M., De Vivo, B., De Vos, W., Dinelli, E., Lima, A., O'Connor, P.J., Salpeteur, I., Tarvainen, T., 2014. Natural radioactive elements U, Th and K in european agricultural and grazing land soil (Chapter 8). In: Reimann, C., Birke, M., Demetriades, A., Filzmoser, P., O'Connor, P. (Eds.), Chemistry of Europe's Agricultural Soils – Part B: General Background Information and Further Analysis of the GEMAS Data Set. Geologisches Jahrbuch (Reihe B103), Schweizerbarth, Hannover, pp. 145–159.

Cristache, C., Comero, S., Locoro, G., Fissiaux, I., Ruiz, A.A., Tóth, G., Gawlik, B.M., 2014. Comparative Study on Open System Digestion vs. Microwave-Assisted Digestion Methods for Trace Element Analysis in Agricultural Soils. Joint Research Centre, Institute for Environment and Sustainability, Luxembourg, p. 38. http://publications.jrc.ec.europa.eu/repository/bitstream/JRC90183/lb-na-26636-en-n.pdf.

Demetriades, A., 2011. Understanding the quality of chemical data from the urban environment – Part 2: measurement uncertainty in the decision-making process (Chapter 6). In: Johnson, C.C., Demetriades, A., Locutura, J., Ottesen, R.T. (Eds.), Mapping the Chemical Environment of Urban Areas. John Wiley & Sons Ltd., Chichester, U.K., pp. 77–98. https://doi.org/10.1002/9780470670071.ch6

Demetriades, A., Reimann, C., 2014. Mineral deposits of Europe (Chapter 3). In: Reimann, C., Birke, M., Demetriades, A., Filzmoser, P., O'Connor, P. (Eds.), Geologisches Jahrbuch (Reihe B 103). Schweizerbarth, Hannover, pp. 71–78.

Demetriades, A., Reimann, C., Filzmoser, P., 2014. Evaluation of GEMAS project quality control results (Chapter 6). In: Reimann, C., Birke, M., Demetriades, A., Filzmoser, P., O'Connor, P. (Eds.), Chemistry of Europe's Agricultural Soils – Part A: Methodology and Interpretation of the GEMAS Data Set Geologisches Jahrbuch (Reihe B102). Schweizerbarth, Hannover, pp. 47–60.

De Vos, W., Tarvainen, T., Salminen, R., Reeder, S., De Vivo, B., Demetriades, A., Pirc, S., Batista, M.J., Marsina, K., Ottesen, R.T., O'Connor, P., Bidovec, M., Lima, A., Siewers, U., Smith, B., Taylor, H., Shaw, R., Salpeteur, I., Gregorauskiene, V., Halamić, J., Slaninka, I., Lax, K., Gravesen, P., Birke, M., Breward, N., Ander, E.L., Jordan, G., Duris, M., Klein, P., Locutura, J., Bel-lan, A., Pasieczna, A., Lis, J., Mazreku, A., Gilucis, A., Heitzmann, P., Klaver, G., Petersell, V., 2006. Geochemical Atlas of Europe. Part 2 - Interpretation of Geochemical Maps, Additional Tables, Figures, Maps, and Related Publications. Geological Survey of Finland, Espoo, p. 618. http://weppi.gtk.fi/publ/foregsatlas/.

ECS, 2010. Sludge, Treated Biowaste and Soil - Digestion for the Extraction of Aqua Regia Soluble Fraction of Trace Elements. prEN 16174, CEN/TC400 (Draft). European Committee for Standardisation, Brussels, p. 15. https://www.ecn.nl/docs/society/horizontal/BT_TF151_WI_CSS99025B_Aqua_regia_2992007.pdf.

European Commission, 2017. Study on the Review of the List of Critical Raw Materials: Criticality Assessments. Brussels, 13.9.2017. COM(2017) 490 final, p. 92. http://doi.org/10.2873/876644.

Fay, D., Kramers, G., Zhang, C., McGrath, D., Grennan, E., 2007. Soil Geochemical Atlas of Ireland. Teagasc, Environmental Protection Agency, Wexford, p. 117. https://www.teagasc.ie/media/website/publications/2011/Soil_Geochemical_AtlasofIreland.pdf.

Filzmoser, P., Reimann, C., Birke, M., 2014. Univariate data analysis and mapping (Chapter 8). In: Reimann, C., Birke, M., Demetriades, A., Filzmoser, P., O'Connor, P. (Eds.), Chemistry of Europe's Agricultural Soils – Part A: Methodology and Interpretation of the GEMAS Data Set. Geologisches Jahrbuch (Reihe B102). Schweizerbarth, Hannover, pp. 67–81.

Gál, J., Hursthouse, A., Cuthbert, S., 2007. Bioavailability of arsenic and antimony in soils from an abandoned mining area, Glendinning (SW Scotland). J. Environ. Sci. Health Part A Toxic Hazard.Subst. Environ. Eng. 42, 1263–1274.

Garrett, R.G., Reimann, C., Smith, D.B., Xie, X., 2008. From geochemical prospecting to international geochemical mapping: a historical overview. Geochem. Explor. Environ. Anal. 8, 205–217.

Günther, A., Reichenbach, P., Malet, J.-P., Van Den Eeckhaut, M., Hervás, J., Dashwood, C., Guzzetti, F., 2013. Tier-based Approaches for Landslide Susceptibility Assessment in Europe Landslides, vol. 10, pp. 529–546.

Hockmann, K., Schulin, R., 2013. Leaching of antimony from contaminated soils. In: Selim, H.M. (Ed.), Competitive Sorption and Transport of Heavy Metals in Soils and Geological Media. CRC Press, Boca Raton, pp. 119–145.

Hu, Z., Gao, S., 2008. Upper crustal abundances of trace elements: a revision and update. Chem. Geol. 253, 205–221.

Hubbert, M.K., 1982. Techniques of prediction as applied to production of oil and gas. In: Gass, S.I. (Ed.), Oil and Gas Supply. US Department of Commerce, NBS Special Publication 631. May 1982.

Johnson, C.A., Moench, H., Wersin, P., Kugler, P., Wenger, C., 2005. Solubility of antimony and other elements in samples taken from shooting ranges. J. Environ. Qual. 34, 248–254.

Jordan, G., Petrik, A., De Vivo, B., Albanese, S., Demetriades, A., Sadeghi, M., The GEMAS Project Team, 2018. GEMAS: spatial analysis of the Ni distribution on a continental-scale using digital image processing techniques on European agricultural soil data. J. Geochem. Explor. 143–157.

Kabata-Pendias, A., Mukherjee, A.B., 2007. Trace Elements from Soil to Human. Springer Verlag, Berlin, Heidelberg, p. 550.

Koutsospyros, A., Braida, W., Christodoulatos, C., Dermatas, D., Strigul, N., 2006. A review of tungsten: from environmental obscurity to scrutiny. J. Hazard Mater. 136, 1–19.

Ladenberger, A., Andersson, M., Reimann, C., Tarvainen, T., Filzmoser, P., Uhlbäck, J., Morris, G., Sadeghi, M., 2013. Geochemical Mapping of Agricultural Soils and Grazing Land (GEMAS) in Norway, Finland and Sweden – Regional Report. SGU-rapport 2012:17. Geological Survey of Sweden, p. 160. http://resource.sgu.se/produkter/sgurapp/s1217-rapport.pdf. https://www.researchgate.net/publication/260872161_Geochemical_mapping_of_agricultural_soils_and_grazing_land_GEMAS_in_Norway_Finland_and_Sweden_-_regional_report.

Ladenberger, A., Demetriades, A., Reimann, C., Birke, M., Sadeghi, M., Uhlback, J., Andersson, M., Jonsson, E., the GEMAS Project Team, 2015. GEMAS: indium in agricultural and grazing land soil of Europe – its source and geochemical distribution patterns. J. Geochem. Explor. 154, 61–80.

Ladenberger, A., Uhlbäck, J., Andersson, M., Reimann, C., Tarvainen, T., Morris, G., Sadeghi, M., Eklund, M., Filzmoser, P., 2014. Elemental Patterns in Agricultural and Grazing Land soil in Norway, Finland and Sweden: what have we learned from continental-scale mapping? (Chapter 14) In: Reimann, C., Birke, M., Demetriades, A., Filzmoser, P., O'Connor, P. (Eds.), Chemistry of Europe's Agricultural Soils – Part B: General Background Information and Further Analysis of the GEMAS Data Set. Geologisches Jahrbuch (Reihe B103). Schweizerbarth, Hannover, pp. 235–251.

Lambert, I., Durrheim, R., Godoy, M., Kota, M., Leahy, P., Ludden, J., Nickless, E., Oberhaensli, R., Anjian, W., Williams, N., 2013. Resourcing Future Generations: a proposed new IUGS initiative. Episodes 36, 82–86.

Locutura, J., Bel-lan, A., García, C.A., Martínez, S., 2012. Atlas Geoquímico de España. Instituto Geológico y Minero de España, Madrid, p. 592 pp. (A3 size). http://www.igme.es/actividadesIGME/lineas/CartoGeo/geoquimica/geoquimicaIng.htm.

Meinert, L.D., Robinson, G.R., Nassar, N.T., 2016. Mineral resources: reserves, peak production and the future. Resources 5, 14.

Millot, R., Vigier, N., Gaillardet, J., 2010. Behaviour of lithium and its isotopes during weathering in the Mackenzie Basin, Canada. Geochem. Cosmochim. Acta 74, 3897–3912.

Négrel, Ph, Sadeghi, M., Ladenberger, A., Reimann, C., Birke, M., the GEMAS Project Team, 2015. Geochemical fingerprinting and sources discrimination in soils and sediments at continental scale. Chem. Geol. 396, 1–15.

Négrel, Ph, Ladenberger, A., Reimann, C., Birke, M., Sadeghi, M., the GEMAS Project Team, 2016. GEMAS: source, distribution patterns and geochemical behavior of Ge in agricultural and grazing land soils at European continental scale. Appl. Geochem. 72, 113–124.

Négrel, Ph, De Vivo, B., Reimann, C., Ladenberger, A., Cicchella, D., Albanese, S., Birke, M., De Vos, W., Dinelli, E., Lima, A., O'Connor, P.J., Salpeteur, I., Tarvainen, T., the GEMAS Project Team, 2018. U-Th signatures of agricultural soil at the European continental scale (GEMAS): distribution, weathering patterns and processes controlling their concentrations. Sci. Total Environ. 622–623, 1277–1293.

Négrel, Ph, Ladenberger, A., Reimann, C., Birke, M., Sadeghi, M., the GEMAS Project Team, 2018. Distribution of Rb, Ga and Cs in agricultural land soils at European continental scale (GEMAS): implications for weathering conditions and provenance. Chem. Geol. 479, 188–203.

Nickless, E., Ali, S., Arndt, N., Brown, G., Demetriades, A., Durrheim, R., Enriquez, M.A., Giurco, D., Kinnaird, J., Littleboy, A., Masotti, F., Meinert, L., Nyanganyura, D., Oberhänsli, R., Salem, J., Schneider, G., Yakovleva, N., 2015. Resourcing Future Generations: A Global Effort to Meet the World's Future Needs Head-On. International Union of Geological Sciences, p. 76. http://iugs.org/uploads/RFG%20Report-sm.pdf.

Ottesen, R.T., Birke, M., Finne, T.E., Gosar, M., Locutura, J., Reimann, C., Tarvainen, T., the GEMAS Project team, 2013. Mercury in European agricultural and grazing land soils. Appl. Geochem. 33, 1–12.

Pawlowsky-Glahn, V., Buccianti, A., 2011. Compositional Data Analysis: Theory and Applications. Wiley, Chichester, p. 378.

Plant, J.A., Breward, N., Forrest, M.D., Smith, R.T., 1989. The gold pathfinder elements As, Sb and Bi: their distribution and significance in the south-west Highlands of Scotland. Trans. Inst. Min. Metall. 98, B91–B101.

Poňavič, M., Scheib, A., 2014. Distribution of Selenium in european agricultural and grazing land soil (Chapter 7). In: Reimann, C., Birke, M., Demetriades, A., Filzmoser, P., O'Connor, P. (Eds.), Chemistry of Europe's Agricultural Soils – Part B: General Background Information and Further Analysis of the GEMAS Data Set. Geologisches Jahrbuch (Reihe B103). Schweizerbarth, Hannover, pp. 131–144.

Rawlins, B.G., McGrath, S.P., Scheib, A.J., Breward, N., Cave, M., Lister, T.R., Ingham, M., Gowing, C., Carter, S., 2012. The Advanced Soil Geochemical Atlas of England and Wales. British Geological Survey, Nottingham, UK, p. 227.

Reimann, C., Siewers, U., Tarvainen, T., Bityukova, L., Eriksson, J., Giucis, A., Gregorauskienė, V., Lukashev, V.K., Matinian, N.N., Pasieczna, A., 2003. Agricultural Soils in Northern Europe - A Geochemical Atlas (Baltic Soil Survey), Geologisches Jahrbuch Sonderhefte Reihe D, Heft 5. Schweizerbart Science Publishers, Stuttgart, p. 279.

Reimann, C., Arnoldussen, A., Englmaier, P., Filzmoser, P., Finne, T.E., Garrett, R.G., Koller, F., Nordgulen, Ø., 2007. Element concentrations and variations along a 120

km long transect in south Norway – anthropogenic *vs.* geogenic *vs.* biogenic element sources and cycles. Appl. Geochem. 22, 851–871.
Reimann, C., Melezhik, V., Niskavaara, H., 2007. Low-density regional geochemical mapping of gold and palladium highlighting the exploration potential of northernmost Europe. Econ. Geol. 102, 327–334.
Reimann, C., Demetriades, A., Eggen, O.A., Filzmoser, P., The EuroGeoSurveys Geochemistry Expert Group, 2009. The EuroGeoSurveys Geochemical Mapping of Agricultural and Grazing Land Soils Project (GEMAS) – Evaluation of Quality Control Results of Aqua Regia Extraction Analysis. NGU report 2009.049. Geological Survey of Norway, Trondheim, p. 94. http://www.ngu.no/upload/Publikasjoner/Rapporter/2009/2009_049.pdf.
Reimann, C., Matschullat, J., Birke, M., Salminen, R., 2010. Antimony in the environment: lessons from geochemical mapping. Appl. Geochem. 25, 175–198.
Reimann, C., Demetriades, A., Eggen, O.A., Filzmoser, P., EuroGeoSurveys Geochemistry Working Group, 2011. The EuroGeoSurveys Geochemical Mapping of Agricultural and Grazing Land Soils Project (GEMAS) – Evaluation of Quality Control Results of Total C and S, Total Organic Carbon (TOC), Cation Exchange Capacity (CEC), XRF, pH, and Particle Size Distribution (PSD) Analysis. NGU Report 2011.043. Geological Survey of Norway, Trondheim, p. 92. http://www.ngu.no/upload/Publikasjoner/Rapporter/2011/2011_043.pdf.
Reimann, C., Caritat, P. de, GEMAS Project Team, NGSA Project Team, 2012. New soil composition data for Europe and Australia: demonstrating comparability, identifying continental-scale processes and learning lessons for global geochemical mapping. Sci. Total Environ. 416, 239–252.
Reimann, C., Flem, B., Fabian, K., Birke, M., Ladenberger, A., Négrel, Ph, Demetriades, A., Hoogewerff, J., the GEMAS Project Team, 2012. Lead and lead isotopes in agricultural soils of Europe - the continental perspective. Appl. Geochem. 27, 532–542.
Reimann, C., Demetriades, A., Birke, M., Eggen, O.A., Filzmoser, P., Kriete, C., EuroGeoSurveys Geochemistry Expert Group, 2012. The EuroGeoSurveys Geochemical Mapping of Agricultural and Grazing Land Soils Project (GEMAS) – Evaluation of Quality Control Results of Particle Size Estimation by MIR Prediction, Pb-Isotope and MMI® Extraction Analyses and Results of the GEMAS Ring Test for the Standards Ap and Gr. NGU report 2012.051. Geological Survey of Norway, Trondheim, p. 136. http://www.ngu.no/upload/Publikasjoner/Rapporter/2012/2012_051.pdf.
Reimann, C., Filzmoser, P., Fabian, K., Hron, K., Birke, M., Demetriades, A., Dinelli, E., Ladenberger, A., the GEMAS Project Team, 2012. The concept of compositional data analysis in practice - total major element concentrations in agricultural and grazing land soils of Europe. Sci. Total Environ. 426, 196–210.
Chemistry of Europe's agricultural soils – Part A: methodology and interpretation of the GEMAS dataset. In: Reimann, C., Birke, M., Demetriades, A., Filzmoser, P., O'Connor, P. (Eds.), 2014. Geologisches Jahrbuch (Reihe B). Schweizerbarth, Stuttgart, p. 528.
Chemistry of Europe's agricultural soils – Part B: general background information and further analysis of the GEMAS dataset. In: Reimann, C., Birke, M., Demetriades, A., Filzmoser, P., O'Connor, P. (Eds.), 2014. Geologisches Jahrbuch (Reihe B). Schweizerbarth, Stuttgart, p. 352.
Reimann, C., Ladenberger, A., Birke, M., Caritat, P. de, 2016. Low density geochemical mapping and mineral exploration: application of the mineral system concept. Geochem. Explor. Environ. Anal. 16, 48–61.
Roda-Robles, E., Pesquera, A., Gil-Crespo, P.P., Vieira, R., Lima, A., Garate-Olave, I., Martins, T., Torres-Ruiz, J., 2016. Geology and mineralogy of Li mineralization in the central iberian zone (Spain and Portugal). Mineral. Mag. 80, 103–126.
Sadeghi, M., Petrosino, P., Ladenberger, A., Albanese, S., Andersson, M., Morris, G., Lima, A.M., De Vivo, B., the GEMAS Project Team, 2013. Ce, La and Y concentrations in agricultural and grazing-land soils of Europe. J. Geochem. Explor. 133, 202–213.
Salminen, R., Tarvainen, T., Demetriades, A., Duris, M., Fordyce, F.M., Gregorauskiene, V., Kahelin, H., Kivisilla, J., Klaver, G., Klein, P., Larson, J.O., Lis, J., Locutura, J., Marsina, K., Mjartanova, H., Mouvet, C., O'Connor, P., Odor, L., Ottonello, G., Paukola, T., Plant, J.A., Reimann, C., Schermann, O., Siewers, U., Steenfelt, A., Van Der Sluys, J., Williams, L., 1998. FOREGS Geochemical Mapping Field Manual, vol. 47. Geological Survey of Finland, Espoo, Guide, p. 36. http://tupa.gtk.fi/julkaisu/opas/op_047.pdf.
Salminen, R., Batista, M.J., Bidovec, M., Demetriades, A., De Vivo, B., De Vos, W., Ďuriš, M., Gilucis, A., Gregorauskienë, V., Halamiä, J., Heitzmann, P., Lima, A., Jordan, G., Klaver, G., Klein, P., Lis, J.z., Locutura, J., Marsina, K., Mazreku, A., O'Connor, P., Olsson, S.Å., Ottesen, R.T., Petersell, V., Plant, J.A., Reeder, S., Salpeteur, I., Sandström, H., Siewers, U., Steenfelt, A., Tarvainen, T., 2005. Geochemical Atlas of Europe. Part 1 – Background Information, Methodology and Maps. Geological Survey of Finland, Espoo, p. 525. http://weppi.gtk.fi/publ/foregsatlas/.
Scheib, A.J., Flight, D.M.A., Birke, M., Tarvainen, T., Locutura, J., GEMAS Project Team, 2012. The geochemistry of niobium and its distribution and relative mobility in agricultural soils of Europe. Geochem. Explor. Environ. Anal. 12, 293–302.
Smith, D.B., Reimann, C., 2008. Low-density geochemical mapping and the robustness of geochemical patterns. Geochem. Explor. Environ. Anal. 8, 219–227.
Smith, D.B., Cannon, W.F., Woodruff, L.G., Solano, F., Kilburn, J.E., Fey, D.L., 2013. Geochemical and Mineralogical Data for Soils of the Conterminous United States, Data Series 801. U.S. Geological Survey, Reston, p. 19.
Smith, D.B., Cannon, W.F., Woodruff, L.G., Solano, F., Ellefsen, K.J., 2014. Geochemical and Mineralogical Maps for Soils of the Conterminous United States, Open-File Report 2014–1082. U.S. Geological Survey, Denver, p. 386.
Takahashi, T., Shozugawa, K., Matsuo, M., 2010. Contribution of amorphous iron compounds to adsorptions of pentavalent antimony by soils. Water Air Soil Pollut. 208, 165–172.
Tarvainen, T., Albanese, S., Birke, M., Ponavic, M., Reimann, C., the GEMAS Project Team, 2013. Arsenic in agricultural and grazing land soils of Europe. Appl. Geochem. 28, 2–10.
Tardy, Y., Krempp, G., Trauth, N., 1972. Le lithium dans les minéraux argileux des sédiments et des sols. Geochem. Cosmochim. Acta 36, 397–412.
Teske, S. (Ed.), 2019. Achieving the Paris Climate Agreement Goals: Global and Regional 100% Renewable Energy Scenarios with Non-energy GHG Pathways for +1.5°c and +2°C. Springer Open, p. 491. https://doi.org/10.1007/978-3-030-05843-2.
Tóth, G., Hermann, T., Szatmári, G., Pásztor, L., 2016. Maps of heavy metals in the soils of the European Union and proposed priority areas for detailed assessment. Sci. Total Environ. 565, 1054–1062.
UNEP, 2009. Critical Metals for Future Sustainable Technologies and Their Recycling Potential. UNEP, DTI/1202/PA, Paris, p. 81. http://www.unep.fr/shared/publications/pdf/DTIx1202xPA-Critical%20Metals%20and%20their%20Recycling%20Potential.pdf.
Wedepohl, K.H., Exec (Eds.), 1978. Handbook of Geochemistry, II/5. Springer-Verlag, Berlin, Heidelberg, New York, p. 4400+.
Xie, X., Ren, T., Sun, H., 2012. Geochemical Atlas of China. Institute of Geophysical and Geochemical Exploration, Langfang, China, p. 135.
Zeeberg, J.J., 1998. The European sand belt in Eastern Europe – and comparison of Late Glacial dune orientation with GCM simulation results. Boreas 27, 127–139.